

On the motion of slightly rarefied gas induced by a discontinuous surface temperature

Satoshi Taguchi^{1,2,†} and Tetsuro Tsuji^{1,2}

¹Department of Advanced Mathematical Sciences, Graduate School of Informatics, Kyoto University, Kyoto 606-8501, Japan

²Research Project of Fluid Science and Engineering, Advanced Engineering Research Center, Kyoto University, Kyoto 606-8501, Japan

(Received 21 December 2019; revised 11 March 2020; accepted 22 April 2020)

The motion of a slightly rarefied gas in a long straight two-dimensional channel caused by a discontinuous surface temperature is investigated on the basis of kinetic theory with a special interest in the fluid-dynamic description. More precisely, the channel is longitudinally divided into two parts and each part is kept at a uniform temperature different from each other, so that the surface temperature of the whole channel has a jump discontinuity at the junction. Under the assumption that the amount of jump in the surface temperature is small, the steady behaviour of the gas induced in the channel is studied on the basis of the linearized Boltzmann equation and the diffuse reflection boundary condition in the case where the Knudsen number, defined by the ratio of the molecular mean free path and the width of the channel, is small. Using a matched asymptotic expansion method combined with Sone's asymptotics, a Stokes system describing the overall macroscopic behaviour of the gas inside the channel is derived, with a new feature of the 'slip boundary condition' for the flow velocity due to the jump discontinuity in the surface temperature of the channel. This condition takes the form of a diverging singularity with source and sink located at the point of discontinuity, with a multiplicative factor determined through the analysis of a spatially two-dimensional Knudsen-layer (or a Knudsen-zone) problem. Some numerical demonstrations based on the Bhatnagar–Gross–Krook equation are also presented.

Key words: non-continuum effects, kinetic theory

1. Introduction

In a gas in small-scale systems or in a gas with low pressure, the molecular mean free path is often no longer negligible in comparison with the characteristic system size. In such a gas (or in a rarefied gas), the temperature field causes a steady motion of the gas in the absence of external forces (e.g. gravity). A well-known example is the thermal-creep flow (or thermal transpiration) induced over a surface with a non-uniform temperature distribution (Kennard 1938; Sone 1966; Sone & Yamamoto 1968;

† Email address for correspondence: taguchi.satoshi.5a@kyoto-u.ac.jp

Loyalka 1969; Niimi 1971; Ohwada, Sone & Aoki 1989a,b; Sharipov 2002; Takata & Funagane 2011). The thermally induced flows have been an active research area of rarefied gas dynamics (or kinetic theory of gases) in the last half-century (see Sone (2007) and the references therein).

We shall hereafter focus on steady flows. As a kinetic effect, one requires kinetic theory (i.e. the Boltzmann equation) for accurate descriptions of the thermally induced flows. However, when the molecular mean free path is sufficiently small compared with the characteristic size of the system (i.e. near-continuum regime), a macroscopic system can be derived from the Boltzmann system and the thermally induced flows are conveniently described by suitable fluid-dynamic-type equations and their boundary conditions. This theory, intended to cover not only the thermally induced flows but also other kinetic effects, such as the shear slip, the temperature jump, and so on, is called the generalized slip-flow (GSF) theory, which was developed notably by Sone (1969, 1971, 2002, 2007). The theory has been applied to various thermally induced flows (e.g. Sone 2007; Li, Liang & Ye 2014).

The GSF theory assumes that the boundary shape of bodies and the boundary condition on the bodies are smooth. To be more specific, the latter means that the surface temperature as well as the surface velocity of each body should be a smooth function of the position on the body. Therefore, the theory does not apply to the case where the boundary temperature has a jump discontinuity and/or to the case where the boundary shape has a sharp edge.

In the meantime, thermally induced flows caused by a discontinuous surface temperature and/or a sharp edge have also been investigated in the literature. For example, the thermal edge flow, induced around a uniformly heated flat plate with a sharp edge, was discovered (Aoki, Sone & Masukawa 1995; Sone & Yoshimoto 1997) and applied to a vacuum pump (the thermal edge pump; Sugimoto & Sone 2005; Sone 2007). Also, flows induced over a flat plate with different surface temperatures on both sides were investigated (Ketsdever *et al.* 2012; Taguchi & Aoki 2012) in connection with thermophoretic effects (Ketsdever *et al.* 2012). It was shown that the parallel alignment of flat plates also have a pumping effect when appropriately heated (Taguchi & Aoki 2015; Baier *et al.* 2017). Actually, flows related to discontinuous surface temperature have been a subject of recent studies, such as thermally driven pumps (e.g. Donkov *et al.* 2011; Lotfian & Roohi 2019) and thermophoresis (Aoki, Takata & Tomota 2014) (see also Baier *et al.* (2018)). Despite its theoretical and practical interest, however, the understanding of these flows is far behind due to the lack of general theory.

Given these situations, it is important to examine whether one can extend the GSF theory to the case of a discontinuous surface temperature and/or a non-smooth boundary shape. The purpose of the present paper is to give an affirmative answer to this question in the simplest case. More specifically, we consider a slightly rarefied gas in a long straight two-dimensional channel whose surface temperature has a jump discontinuity. With the assumption of small jumps, we derive a system of Stokes equations for the overall (stationary) flow field in the channel together with a ‘slip boundary condition’, which is intended to describe a flow due to the discontinuous surface temperature. This slip condition, however, is far from the conventional slip condition and takes the form of a source/sink singularity which diverges in approaching the point of discontinuity.

The rest of the paper is organized as follows. In § 2, as a preparation for the subsequent analysis, we consider a rarefied gas flow between two parallel plates with a smooth surface temperature distribution, and investigate its asymptotic behaviour

for small Knudsen numbers using conventional Sone’s method. In § 3, we consider a rarefied gas flow between two parallel plates with a discontinuous surface temperature and discuss its asymptotic behaviour for small Knudsen numbers based on the result of § 2. We show that Sone’s asymptotics obtained in § 2 breaks down in the vicinity of the discontinuous point, and therefore a local correction is needed there. We use this local correction to derive the desired boundary condition for the flow velocity. Section 4 presents some numerical demonstrations to support our analytical prediction. Section 5 is the concluding remarks.

2. Behaviour of a slightly rarefied gas between two parallel plates with a smooth temperature distribution

As a preliminary, we consider a gas confined between two parallel plates with a smooth temperature distribution and investigate its behaviour for small Knudsen numbers. In the following, we denote the characteristic length by L , the characteristic density of the gas by ρ_0 , the characteristic temperature by T_0 and the characteristic pressure by $p_0 = \rho_0 RT_0$, where R is the specific gas constant, i.e. $R = k_B/m$ with k_B and m being the Boltzmann constant and the mass of a molecule, respectively.

2.1. Problem

Let Lx_i ($i = 1, 2, 3$) be the space rectangular coordinate system. We consider a rarefied gas confined between two parallel plates located at $Lx_1 = \pm La$, where a is a positive constant. The temperatures of the two plates, which are constant in time, are the same and the temperature distribution is given by $T_0(1 + \tau_w)$, where $\tau_w = \tau_w(x_2, x_3)$ is assumed to be a smooth function of x_2 and x_3 . There is no pressure gradient imposed on the gas nor external force. We investigate the steady behaviour of the gas in the domain $D = \{(x_1, x_2, x_3) \mid -a < x_1 < a, -\infty < x_2 < \infty, -\infty < x_3 < \infty\}$ based on the Boltzmann equation with the diffuse reflection boundary condition on the plate surface, under the assumption that $|\partial\tau_w/\partial x_i|$ is so small that the equation and boundary conditions can be linearized around the reference equilibrium state at rest. In particular, we investigate the steady behaviour of the gas when the Knudsen number of the system $Kn = \ell_0/L$ is small. Here, ℓ_0 is the mean free path of the gas molecules in the equilibrium state at rest with temperature T_0 and density ρ_0 . Throughout the paper, we use the symbol

$$\varepsilon = \frac{\sqrt{\pi}}{2} Kn \tag{2.1}$$

to denote the small parameter of the problem.

To illustrate the physical situation that can be described by the above problem, we give two particular examples for τ_w . The simplest example is the case where $\partial\tau_w/\partial x_i$ is constant, say $(\partial\tau_w/\partial x_2, \partial\tau_w/\partial x_3) = (\beta_1, 0)$ with β_1 being a (small) constant. In this case, the problem is nothing but the classical thermal transpiration between two parallel plates (Niimi 1971; Ohwada *et al.* 1989a; Sone 2007). Another example is given by a periodic function, say $\tau_w = \beta_2 g(x_2)$, where β_2 is a (small) constant and $g(x_2)$ with $dg/dx_2 = O(1)$ is periodic in x_2 . In this case, we are concerned with the spatially periodic motion of a gas thermally induced in the channel.

2.2. Basic equations

Let the molecular velocity be denoted by $(2RT_0)^{1/2}\zeta_i$ and the velocity distribution function by $\rho_0(2RT_0)^{-3/2}(1 + \phi(x_i, \zeta_i))E$, where $E = E(\zeta_i) := \pi^{-3/2} \exp(-\zeta_i^2)$ is the

normalized absolute Maxwellian. The linearized Boltzmann equation for the present steady problem is then written as

$$\zeta_i \partial_i \phi = \frac{1}{\varepsilon} \mathcal{L}(\phi), \tag{2.2}$$

where $\partial_i = \partial/\partial x_i$ and \mathcal{L} is the linearized collision operator, whose explicit form is omitted here (see, e.g. Sone 2007, chap. 1). The diffuse reflection boundary condition on the plates are given as follows:

$$\begin{aligned} \phi &= 2\sqrt{\pi} \int_{\zeta_1 \leq 0} |\zeta_1| \phi E d\zeta + (\zeta_j^2 - 2)\tau_w, \quad \zeta_1 \geq 0, \\ (x_1 &= \mp a, -\infty < x_2 < \infty, -\infty < x_3 < \infty), \end{aligned} \tag{2.3}$$

where $d\zeta = d\zeta_1 d\zeta_2 d\zeta_3$.

Next, we introduce the macroscopic quantities. Let $\rho_0(1 + \omega(x_i))$ denote the mass density, $(2RT_0)^{1/2}u_i(x_i)$ the flow velocity, $T_0(1 + \tau(x_i))$ the temperature, and $p_0(1 + P(x_i))$ the pressure of the gas. Then, ω , u_i , τ and P are expressed in terms of ϕ as the moments with respect to the molecular velocity, i.e.

$$\omega = \langle \phi \rangle, \quad u_i = \langle \zeta_i \phi \rangle, \tag{2.4a}$$

$$\tau = \frac{2}{3} \langle (\zeta_j^2 - \frac{3}{2}) \phi \rangle, \quad P = \frac{2}{3} \langle \zeta_j^2 \phi \rangle = \omega + \tau. \tag{2.4b}$$

Here, the bracket symbol means the following integral:

$$\langle f \rangle = \int f(\zeta_i) E d\zeta, \tag{2.5}$$

where the range of integration spans over the whole velocity space.

2.3. Summary of the asymptotic analysis for small ε

We investigate the behaviour of the gas between the plates in the case where $\varepsilon \ll 1$, following the method of Sone (the asymptotic analysis of the Boltzmann equation for small ε (Sone 2002, 2007)). Since the procedure is explained in detail in the references, we briefly explain the derivation of the fluid-dynamic-type system to the first order of ε for the subsequent discussions.

2.3.1. Hilbert solution and fluid-dynamic-type equations

First, putting aside the boundary condition, we consider the solution of the linearized Boltzmann equation (2.2) which varies moderately in space. This type of solution is called the Hilbert solution and is designated by attaching the subscript H , i.e. $\partial_i \phi_H = O(\phi_H)$. We seek ϕ_H in the form of a simple expansion in ε :

$$\phi_H = \phi_{H0} + \phi_{H1}\varepsilon + \dots \tag{2.6}$$

Corresponding to this expansion, the macroscopic quantities are also expanded in a power series of ε :

$$h_H = h_{H0} + h_{H1}\varepsilon + \dots, \quad (h = \omega, u_i, \tau, P). \tag{2.7}$$

The relation between h_{Hm} and ϕ_{Hm} ($m = 0, 1, \dots$) is simply obtained as follows:

$$\omega_{Hm} = \langle \phi_{Hm} \rangle, \quad u_{iHm} = \langle \zeta_i \phi_{Hm} \rangle, \tag{2.8a}$$

$$\tau_{Hm} = \frac{2}{3} \langle (\zeta_j^2 - \frac{3}{2}) \phi_{Hm} \rangle, \quad P_{Hm} = \frac{2}{3} \langle \zeta_j^2 \phi_{Hm} \rangle. \tag{2.8b}$$

Substituting the above expansion for ϕ_H into (2.2) and arranging the terms of the same order in ε , we obtain the following sequence of linear integral equations for ϕ_{Hm} :

$$\mathcal{L}(\phi_{H0}) = 0, \tag{2.9a}$$

$$\mathcal{L}(\phi_{Hm}) = \zeta_i \partial_i \phi_{Hm-1}, \quad (m \geq 1). \tag{2.9b}$$

These equations can be solved successively from the lowest order, provided that the following solvability conditions are satisfied (Sone 2002, 2007):

$$\partial_i \langle \psi_j \zeta_i \phi_{Hm-1} \rangle = 0, \quad (m = 1, 2, \dots). \tag{2.10}$$

Here, $j \in \{0, 1, \dots, 4\}$ and $(\psi_0, \psi_i, \psi_4) = (1, \zeta_i, \zeta_j^2)$ are the collision invariants. These solvability conditions provide closed sets of partial differential equations for the macroscopic variables (i.e. fluid-dynamic-type equations). Specifically, the resulting equations are the well-known Stokes set of equations (Sone 2002, 2007), which are summarized as follows:

$$\partial_i P_{H0} = 0, \tag{2.11}$$

$$\partial_i u_{iHm} = 0, \tag{2.12a}$$

$$\gamma_1 \nabla^2 u_{iHm} - \partial_i P_{Hm+1} = 0, \tag{2.12b}$$

$$\nabla^2 \tau_{Hm} = 0, \tag{2.12c}$$

($m = 1, 2, \dots$). Here, γ_1 is the constant (dimensionless viscosity) defined by $\gamma_1 = (2/15) \langle \zeta_j^2 \zeta_k^2 B \rangle$, where $B = B(\zeta)$ is the function introduced below in (2.17b). The numerical value of γ_1 depends on the molecular model. For example, for the hard-sphere (HS) model, the Bhatnagar–Gross–Krook (BGK) model (Bhatnagar, Gross & Krook 1954; Welander 1954) and for the ellipsoidal statistical (ES) model (Holway 1966; Andries *et al.* 2000; Brull 2015), the values are given by

$$\gamma_1 = \begin{cases} 1.270042427, & \text{(HS),} \\ 1, & \text{(BGK),} \\ Pr, & \text{(ES),} \end{cases} \tag{2.13}$$

where Pr is a model parameter whose physical meaning is the Prandtl number. The ES model reduces to the BGK model when $Pr = 1$.

It is worth noting that the density of the gas is determined by the equation of state

$$\omega_{Hm} = P_{Hm} - \tau_{Hm}, \quad (m = 0, 1, 2, \dots). \tag{2.14}$$

Therefore, the leading-order density ω_{H0} is not uniform if the leading-order temperature τ_{H0} is not uniform. In this sense, the fluid is not really ‘incompressible’ although the flow velocity is determined by the Stokes equation for an incompressible fluid.

The solvability conditions being satisfied, the velocity distribution functions ϕ_{Hm} are expressed in terms of $(P_{Hm}, u_{iHm}, \tau_{Hm})$ and the spatial derivatives of $(P_{Hn}, u_{iHn}, \tau_{Hn})$ ($n < m$). For instance, ϕ_{H0} and ϕ_{H1} are given as follows:

$$\phi_{H0} = \phi_{eH0}, \tag{2.15a}$$

$$\phi_{H1} = \phi_{eH1} - \zeta_i A(\zeta)(\partial_i \tau_{H0}) - \frac{1}{2} \zeta_i \zeta_j B(\zeta)(\partial_j u_{iH0} + \partial_i u_{jH0}), \tag{2.15b}$$

where $\zeta = (\zeta_j^2)^{1/2}$,

$$\phi_{eHm} = P_{Hm} + 2\zeta_i u_{iHm} + \left(\zeta_j^2 - \frac{5}{2}\right) \tau_{Hm}, \quad (m = 0, 1, \dots), \tag{2.16}$$

and $A = A(\zeta)$ and $B = B(\zeta)$ are the solutions to the following integral equations:

$$\mathcal{L}(\zeta_i A) = -\zeta_i(\zeta^2 - \frac{5}{2}), \quad \text{with } \langle \zeta^2 A \rangle = 0, \tag{2.17a}$$

$$\mathcal{L}((\zeta_i \zeta_j - (\zeta^2/3)\delta_{ij}) B) = -2(\zeta_i \zeta_j - (\zeta^2/3)\delta_{ij}), \tag{2.17b}$$

where δ_{ij} is the Kronecker delta.

2.3.2. *The Knudsen-layer analysis and the boundary conditions for the fluid-dynamic-type equations*

In the discussion of the Hilbert solution, the boundary condition has not been taken into account. Let us suppose that the leading-order flow velocity u_{iH0} and temperature τ_{H0} take the following values on the boundary:

$$u_{iH0} = 0, \quad \tau_{H0} = \tau_w, \quad (x_1 = \mp a, -\infty < x_2 < \infty, -\infty < x_3 < \infty). \tag{2.18}$$

Then, ϕ_{H0} , being the local Maxwellian, satisfies the diffuse reflection boundary condition (2.3) on $x_1 = \mp a$. However, for higher orders, ϕ_{Hm} ($m \geq 1$) cannot be made to satisfy the boundary condition. This is because the Hilbert solution was obtained under the restriction of moderate variations in all spatial directions. Therefore, to construct the solution satisfying the boundary condition, we need to introduce a boundary layer in which the solution is allowed to change abruptly in the direction normal to the boundary. This boundary layer adjacent to the walls $x_1 = \mp a$ is called the Knudsen layer and the correction to the Hilbert solution in the Knudsen layer is called the Knudsen-layer correction (Sone 2002, 2007).

As is well known, the so-called slip/jump boundary conditions are derived from the Knudsen-layer analysis, whose general procedure is explained in detail in Sone (2002, 2007). In the present study, we repeat the derivation because we will require the information on the velocity distribution function in the Knudsen layer.

We seek the solution in the form

$$\phi = \phi_H + \phi_K. \tag{2.19}$$

Here, ϕ_K represents the correction to the Hilbert solution (Knudsen-layer correction) and the length scale of variation of ϕ_K in the direction normal to the boundary is assumed to be of the order of ε , i.e.

$$\partial_1 \phi_K = O(\phi_K/\varepsilon). \tag{2.20}$$

In order to analyse the Knudsen layers adjacent to the boundary $x_1 = -a$ and $x_1 = a$ in a unified way, we introduce new variables (η, ζ_n) by

$$x_1 = \mp a \pm \varepsilon \eta, \quad \zeta_n = \pm \zeta_1, \quad (\text{near } x_1 = \mp a), \tag{2.21}$$

where $\eta(\geq 0)$ is the stretched coordinate in the direction normal to the boundary. With these variables, we put

$$\phi_K = \phi_K(\eta, x_2, x_3, \zeta_n, \zeta_2, \zeta_3). \tag{2.22}$$

Then, ϕ_K satisfies the following equation:

$$\zeta_n \partial_\eta \phi_K - \mathcal{L}(\phi_K) = -\varepsilon(\zeta_2 \partial_2 + \zeta_3 \partial_3) \phi_K, \tag{2.23}$$

where $\partial_\eta = \partial/\partial\eta$. We further expand ϕ_K in a power series of ε , i.e.

$$\phi_K = \phi_{K1} \varepsilon + \phi_{K2} \varepsilon^2 + \dots \tag{2.24}$$

Note that the expansion starts from ε order, since there is no correction required for ϕ_{H0} and thus $\phi_K = O(\varepsilon)$. Substituting this expansion into (2.23) and arranging the terms of the same order of ε , one can derive a sequence of equations for ϕ_{Km} . On the other hand, the boundary condition for ϕ_{Km} at $\eta=0$ is obtained from the requirement that $\phi_{Hm} + \phi_{Km}$ satisfies the diffuse reflection boundary condition (2.3). Finally, we require that ϕ_{Km} approaches zero rapidly as $\eta \rightarrow \infty$ since it is a correction (matching condition).

We summarize the equation and boundary condition for ϕ_{K1} thus obtained:

$$\zeta_n \partial_\eta \phi_{K1} = \mathcal{L}(\phi_{K1}), \tag{2.25}$$

$$\begin{aligned} \phi_{K1} = & -(\zeta^2 - 2)(\tau_{H1})_0 + \zeta_n A(\zeta) n_i (\partial_i \tau_{H0})_0 \\ & + \bar{\zeta}_i [-2(u_{iH1})_0 + A(\zeta) (\partial_i \tau_{H0})_0 + \zeta_n B(\zeta) n_j (\partial_j u_{iH0} + \partial_i u_{jH0})_0] \\ & + K(\phi_{K1}), \quad \zeta_n > 0, \eta = 0, \end{aligned} \tag{2.26}$$

$$\phi_{K1} \rightarrow 0, \quad (\text{rapidly}), \quad \eta \rightarrow \infty. \tag{2.27}$$

Here, $n_i = (\pm 1, 0, 0)$ is the unit normal vector on the boundary $x_1 = \mp a$ pointing to the gas, $\bar{\zeta}_i = \zeta_i - \zeta_n n_i = \zeta_j (\delta_{ij} - n_i n_j)$, and the symbol $(\cdot)_0$ indicates the value on the boundary ($\eta = 0$ or $x_1 = \mp a$). Further, we have introduced the (linear) operator

$$K(\varphi) = 2\sqrt{\pi} \int_{\zeta_1 < 0} |\zeta_1| \varphi(\zeta_1, \zeta_2, \zeta_3) E \, d\zeta, \tag{2.28}$$

for later convenience. Incidentally, the impermeability on the boundary implies

$$(u_{1H1})_0 = 0. \tag{2.29}$$

The boundary condition (2.26) was simplified with the aid of this condition.

The linearity of the problem and the axisymmetry of the operators $\zeta_n \partial_\eta - \mathcal{L}$ and K with respect to the η axis allow us to seek ϕ_{K1} in the form:

$$\begin{aligned} \phi_{K1} = & \varphi_1^{(0)}(\eta, \zeta_n, \zeta) n_i (\partial_i \tau_{H0})_0 \\ & + \bar{\zeta}_i [\varphi_1^{(1)}(\eta, \zeta_n, \zeta) n_j (\partial_j u_{iH0} + \partial_i u_{jH0})_0 + \varphi_2^{(1)}(\eta, \zeta_n, \zeta) (\partial_i \tau_{H0})_0]. \end{aligned} \tag{2.30}$$

Splitting further the constants $(\tau_{H1})_0$ and $(\delta_{ij} - n_i n_j)(u_{jH1})_0$ in (2.26) as

$$(\tau_{H1})_0 = c_1^{(0)} n_i (\partial_i \tau_{H0})_0, \tag{2.31a}$$

$$\begin{aligned} (\delta_{ij} - n_i n_j)(u_{jH1})_0 &= b_1^{(1)} (\delta_{ij} - n_i n_j) n_k (\partial_k u_{jH0} + \partial_j u_{kH0})_0 \\ &\quad + b_2^{(2)} (\delta_{ij} - n_i n_j) (\partial_j \tau_{H0})_0, \end{aligned} \tag{2.31b}$$

we see that $\varphi_1^{(0)} = \varphi_1^{(0)}(\eta, \zeta_n, \zeta)$ and $\varphi_j^{(1)} = \varphi_j^{(1)}(\eta, \zeta_n, \zeta)$ solve the following half-space boundary-value problems:

$$\left. \begin{aligned} (\zeta_n \partial_\eta - \mathcal{L})\varphi_1^{(0)} &= 0, \\ \varphi_1^{(0)} &= -(\zeta^2 - 2)c_1^{(0)} + \zeta_n A(\zeta) + K(\varphi_1^{(0)}), \quad \zeta_n > 0, \eta = 0, \\ \varphi_1^{(0)} &\rightarrow 0, \eta \rightarrow \infty, \end{aligned} \right\} \tag{2.32a}$$

$$\left. \begin{aligned} (\zeta_n \partial_\eta - \mathcal{L}_1)\varphi_j^{(1)} &= -I_j(\eta, \zeta_n, \zeta), \\ \varphi_j^{(1)} &= -2b_j^{(1)} + J_j(\zeta_n, \zeta), \quad \zeta_n > 0, \eta = 0, \\ \varphi_j^{(1)} &\rightarrow 0, \eta \rightarrow \infty, \end{aligned} \right\} \tag{2.32b}$$

where $c_1^{(0)}$ and $b_j^{(1)}$ are constants,

$$I_1 = 0, \quad I_2 = 0, \quad I_3 = \varphi_1^{(0)}(\eta, \zeta_n, \zeta), \tag{2.33a}$$

$$J_1 = \zeta_n B(\zeta), \quad J_2 = A(\zeta), \quad J_3 = 2\zeta_n F(\zeta), \tag{2.33b}$$

and the operator \mathcal{L}_1 is defined by $\mathcal{L}(\bar{\zeta}_i g(\zeta_n, \zeta)) = \bar{\zeta}_i \mathcal{L}_1(g)(\zeta_n, \zeta)$. Note that we have also introduced $\varphi_3^{(1)}$ for later use and that $F = F(\zeta)$ is the solution to

$$\mathcal{L}((\zeta_i \zeta_j - (\zeta^2/3)\delta_{ij}) F(\zeta)) = (\zeta_i \zeta_j - (\zeta^2/3)\delta_{ij}) A(\zeta). \tag{2.34}$$

These problems are the so-called Knudsen-layer problems and it is known that (i) there exists a solution to the problem if and only if the constant $c_1^{(0)}$ or $b_j^{(1)}$ takes a special value; (ii) the solution is unique; (iii) the decay of the solution as $\eta \rightarrow \infty$ is exponentially fast (Bardos, Caflisch & Nicolaenko 1986; Coron, Golse & Sulem 1988; Sone 2007). With the constants $b_j^{(1)}$ ($j = 1, 2$) and $c_1^{(0)}$ thus determined, $(\tau_{H1})_0$ and $(u_{iH1})_0$ satisfy the following conditions on the boundary:

$$(\tau_{H1})_0 = c_1^{(0)} n_i (\partial_i \tau_{H0})_0, \tag{2.35}$$

$$(u_{iH1})_0 n_i = 0, \quad (u_{iH1})_0 t_i = b_1^{(1)} t_i n_j (\partial_j u_{iH0} + \partial_i u_{jH0})_0 + b_2^{(1)} t_i (\partial_i \tau_{H0})_0, \tag{2.36}$$

where t_i is an arbitrary unit vector tangent to the boundary. Equations (2.35) and (2.36) provide the consistent boundary conditions for the Stokes set of equations, (2.12) for $m = 1$.

The constants $b_1^{(1)}$ and $b_2^{(1)}$ are known as the shear-slip and thermal-slip (or the thermal-creep) coefficients, respectively, whereas $c_1^{(0)}$ is known as the temperature-jump coefficient. The numerical values of these constants for the HS model and the BGK model have been known for a long time (Sone 2002, 2007) and are given in table 1. For the ES model, the following relations are known to hold (Takata, Hattori & Hasebe 2016), i.e. $(b_1^{(1)})_{ES}/Pr = (b_1^{(1)})_{BGK}$ and $(b_2^{(1)})_{ES} = (b_2^{(1)})_{BGK}$, where $(\cdot)_{ES}$ and

	Sone (2002, 2007)	HS	BGK	Notes
$c_1^{(0)}$	d_1	2.4001	1.30272	Temperature jump
$b_1^{(1)}$	$-k_0$	1.2540	1.01619	Shear slip
$b_2^{(1)}$	$-K_1$	0.6465	0.38316	Thermal slip
$b_3^{(1)}$	$d_1 K_1 - a_4$	-1.5846	-0.77837	—
$c_1^{(0)} b_2^{(1)} + b_3^{(1)}$	$-a_4$	-0.0330	-0.27922	Thermal stress slip

TABLE 1. The numerical values of slip/jump coefficients under the diffuse reflection boundary condition for an HS gas and for the BGK model (Sone 2002, 2007; Takata & Hattori 2012). The correspondence to the notations in Sone (2002, 2007) are also shown.

$(\cdot)_{BGK}$ mean the values for the ES and BGK models, respectively. The numerical values of $c_1^{(0)}$ and $b_3^{(1)}$ for the ES model with $Pr = 2/3$ can be found in Takata *et al.* (2016) (see also Takata & Hattori 2015).

Finally, we present the Knudsen-layer correction for the macroscopic variables. Corresponding to (2.19), the macroscopic quantities h ($h = \omega, u_i, \tau, P$) are expressed as $h = h_H + h_K$, where h_K is given by (2.4) with $h = h_K$ and $\phi = \phi_K$. Corresponding to the expansion of ϕ_K in ε , we have

$$h_K = h_{K1}\varepsilon + h_{K2}\varepsilon^2 + \dots, \tag{2.37}$$

with

$$\omega_{Km} = \langle \phi_{Km} \rangle, \quad u_{iKm} = \langle \zeta_i \phi_{Km} \rangle, \tag{2.38a}$$

$$\tau_{Km} = \frac{2}{3} \langle (\zeta_j^2 - \frac{3}{2}) \phi_{Km} \rangle, \quad P_{Km} = \frac{2}{3} \langle \zeta_j^2 \phi_{Km} \rangle, \tag{2.38b}$$

($m = 1, 2, \dots$). Since ϕ_{K1} is expressed by (2.30), the direct substitution into (2.38) yields the following expressions for the macroscopic quantities in the Knudsen layer:

$$\omega_{K1} = \Omega_1^{(0)} n_i (\partial_i \tau_{H0})_0, \quad \tau_{K1} = \Theta_1^{(0)} n_i (\partial_i \tau_{H0})_0, \tag{2.39a}$$

$$P_{K1} = (\Omega_1^{(0)} + \Theta_1^{(0)}) n_i (\partial_i \tau_{H0})_0 = \omega_{K1} + \tau_{K1}, \tag{2.39b}$$

$$u_{iK1} n_i = 0, \quad u_{iK1} t_i = Y_1^{(1)} t_i n_j (\partial_j u_{iH0} + \partial_i u_{jH0})_0 + Y_2^{(1)} t_i (\partial_i \tau_{H0})_0, \tag{2.39c}$$

where $\Omega_1^{(0)} = \Omega_1^{(0)}(\eta)$, $\Theta_1^{(0)} = \Theta_1^{(0)}(\eta)$, and $Y_j^{(1)} = Y_j^{(1)}(\eta)$ are defined by

$$\Omega_1^{(0)} = \langle \varphi_1^{(0)} \rangle, \quad \Theta_1^{(0)} = \frac{2}{3} \langle (\zeta^2 - \frac{3}{2}) \varphi_1^{(0)} \rangle, \quad Y_j^{(1)} = \frac{1}{2} \langle (\zeta^2 - \zeta_n^2) \varphi_j^{(1)} \rangle. \tag{2.40a-c}$$

Note that $\langle \zeta_n \varphi_1^{(0)} \rangle = 0$ was used in the derivation of (2.39).

2.4. Summary of Sone’s asymptotics

In this section, we have considered the steady behaviour of a rarefied gas between two parallel plates whose temperature distribution is a smooth function of x_2 and x_3 in the case where the Knudsen number is small. Its velocity distribution functions are expressed as

$$\phi = \phi_{H0} + \varepsilon(\phi_{H1} + \phi_{K1}) + \dots, \tag{2.41}$$

	Sone (2002, 2007)	Definition	Notes
$A(\zeta)$	A	(2.17a)	—
$B(\zeta)$	B	(2.17b)	—
$F(\zeta)$	F	(2.34)	—
$\varphi_1^{(0)}(\eta, \zeta_n, \zeta)$	—	(2.32a)	Temperature jump
$\varphi_1^{(1)}(\eta, \zeta_n, \zeta)$	—	(2.32b)	Shear slip
$\varphi_2^{(1)}(\eta, \zeta_n, \zeta)$	—	(2.32b)	Thermal slip
$\varphi_3^{(1)}(\eta, \zeta_n, \zeta)$	—	(2.32b)	—
$c_1^{(0)}\varphi_2^{(1)} + \varphi_3^{(1)}$	—	—	Thermal stress slip
$(\Omega_1^{(0)}(\eta), \Theta_1^{(0)}(\eta))$	(Ω_1, Θ_1)	(2.40)	Temperature jump
$Y_1^{(1)}(\eta)$	$-Y_0$	(2.40)	Shear slip
$Y_2^{(1)}(\eta)$	$-\frac{1}{2}Y_1$	(2.40)	Thermal slip
$Y_3^{(1)}(\eta)$	$\frac{d_1}{2}Y_1 - Y_{a4}$	(2.40)	—
$c_1^{(0)}Y_2^{(1)} + Y_3^{(1)}$	$-Y_{a4}$	—	Thermal stress slip

TABLE 2. List of universal functions. The correspondence to the notations in Sone (2002, 2007) are also shown.

with

$$\phi_{H0} = \phi_{eH0}, \tag{2.42}$$

$$\phi_{H1} = \phi_{eH1} - \zeta_i A(\zeta) \partial_i \tau_{H0} - \frac{1}{2} \zeta_i \zeta_j B(\zeta) (\partial_i u_{jH0} + \partial_j u_{iH0}), \tag{2.43a}$$

$$\begin{aligned} \phi_{K1} = & \varphi_1^{(0)}(\eta, \zeta_n, \zeta) n_i (\partial_i \tau_{H0})_0 \\ & + \bar{\zeta}_i \varphi_1^{(1)}(\eta, \zeta_n, \zeta) n_j (\partial_j u_{iH0} + \partial_i u_{jH0})_0 + \bar{\zeta}_i \varphi_2^{(1)}(\eta, \zeta_n, \zeta) (\partial_i \tau_{H0})_0, \end{aligned} \tag{2.43b}$$

where ϕ_{eHm} is given by (2.16). In these expressions, A , B , $\varphi_1^{(0)}$, and $\varphi_j^{(1)}$ are universal in the sense that they do not depend on specific problems. On the other hand, the macroscopic variables arising in the velocity distribution functions contain the specific information of the problem under consideration. They are obtained by solving the Stokes system (2.11)–(2.12) under the following boundary conditions on $x_1 = \mp a$:

(1) order ε^0

$$u_{iH0} = 0, \quad \tau_{H0} = \tau_w(x_2, x_3), \tag{2.44}$$

(2) order ε^1

$$\tau_{H1} = c_1^{(0)} n_i \partial_i \tau_{H0}, \tag{2.45a}$$

$$u_{1H1} = 0, \tag{2.45b}$$

$$u_{iH1} t_i = b_1^{(1)} t_i n_j (\partial_j u_{iH0} + \partial_i u_{jH0}) + b_2^{(1)} t_i \partial_i \tau_{H0}. \tag{2.45c}$$

The formulae for the Knudsen-layer corrections are summarized in (2.39). Table 2 summarizes the universal functions.

3. Behaviour of a slightly rarefied gas between two parallel plates with a discontinuous surface temperature

In this section, we discuss the case of a discontinuous surface temperature based on the result obtained in the previous section. Let us denote again by L the reference length, by ρ_0 the reference density, by T_0 the reference temperature, and by $p_0 = \rho_0 R T_0$ the reference pressure, and consider the following problem.

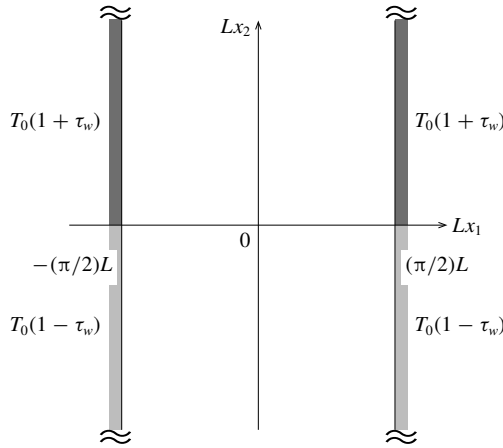


FIGURE 1. Problem.

3.1. Problem

Consider a rarefied gas confined between two parallel plates located at $x_1 = \pm\pi/2$, where Lx_i is the space rectangular coordinate system (figure 1). The two plates are heated (or cooled) non-uniformly in the following way. That is, the upper halves ($x_2 > 0$) are kept at a uniform temperature $T_0(1 + \tau_w)$, while the lower halves ($x_2 < 0$) are kept at another uniform temperature $T_0(1 - \tau_w)$, where τ_w is a constant. Thus, the surface temperature of the channel is discontinuous at $x_2 = 0$ with jump $2T_0|\tau_w|$. There is no pressure gradient imposed on the gas nor external force. We investigate the steady behaviour of the gas in the channel on the basis of the Boltzmann equation and the diffuse reflection boundary condition, under the assumption that $|\tau_w|$ is so small that the equation and boundary conditions can be linearized around the reference equilibrium state at rest. In particular, we pay special attention to the behaviour of the gas when the Knudsen number $Kn = \ell_0/L$, or $\varepsilon = (\sqrt{\pi}/2)Kn$, is small, where ℓ_0 is the mean free path of the gas molecules in the equilibrium state at rest with temperature T_0 and density ρ_0 .

We use the same notations as in the previous section. That is, the velocity distribution function is denoted by $\rho_0(2RT_0)^{-3/2}(1 + \phi(x_1, x_2, \zeta_i))E$. Here, we have assumed that the state of the gas is independent of x_3 . Then, ϕ satisfies the following equation and boundary conditions:

$$\zeta_1 \partial_1 \phi + \zeta_2 \partial_2 \phi = \frac{1}{\varepsilon} \mathcal{L}(\phi), \quad \left(-\frac{\pi}{2} < x_1 < \frac{\pi}{2}, -\infty < x_2 < \infty\right), \quad (3.1)$$

$$\phi = 2\sqrt{\pi} \int_{\zeta_1 < 0} |\zeta_1| \phi E d\zeta \pm (\zeta_j^2 - 2)\tau_w, \quad \zeta_1 > 0, \quad \left(x_1 = -\frac{\pi}{2}, x_2 \geq 0\right), \quad (3.2)$$

$$\phi = 2\sqrt{\pi} \int_{\zeta_1 > 0} |\zeta_1| \phi E d\zeta \pm (\zeta_j^2 - 2)\tau_w, \quad \zeta_1 < 0, \quad \left(x_1 = \frac{\pi}{2}, x_2 \geq 0\right). \quad (3.3)$$

The macroscopic variables, the density $\rho_0(1 + \omega)$, the flow velocity $(2RT_0)^{1/2}u_i$ ($u_3 = 0$), the temperature $T_0(1 + \tau)$, and the pressure $p_0(1 + P)$, are defined as before, and we do not repeat it here (see (2.4)). Note that they are functions of (x_1, x_2) in the present section.

We observe that a solution that is even in (x_1, ζ_1) and odd (antisymmetric) in (x_2, ζ_2) is compatible with the present problem, i.e.

$$\phi(-x_1, x_2, -\zeta_1, \zeta_2, \zeta_3) = \phi(x_1, x_2, \zeta_1, \zeta_2, \zeta_3), \quad (3.4a)$$

$$\phi(x_1, -x_2, \zeta_1, -\zeta_2, \zeta_3) = -\phi(x_1, x_2, \zeta_1, \zeta_2, \zeta_3). \quad (3.4b)$$

Therefore, we may consider the problem in the upper-half domain $x_2 > 0$ by imposing the following reflection condition at $x_2 = 0$:

$$\phi(x_1, 0, \zeta_1, \zeta_2, \zeta_3) = -\phi(x_1, 0, \zeta_1, -\zeta_2, \zeta_3), \quad \zeta_2 > 0. \quad (3.5)$$

In what follows, we denote the restriction of ϕ to $x_2 \geq 0$ by ϕ^\pm and we shall mainly consider ϕ^+ in the sequel. Likewise, h^\pm ($h = \omega, u_i, \tau$ and P) denotes the restriction of h to $x_2 \geq 0$. Once ϕ^+ is obtained, ϕ^- is readily obtained by the relation $\phi^-(x_1, x_2, \zeta_1, \zeta_2, \zeta_3) = -\phi^+(x_1, -x_2, \zeta_1, -\zeta_2, \zeta_3)$.

3.2. Asymptotic matching

We try to investigate the boundary-value problem for ϕ^+ for small $\varepsilon \ll 1$. The idea is to apply the method of matched asymptotic expansion (Dyke 1975; Taguchi 2015; Taguchi & Suzuki 2017) by regarding Sone's asymptotic solution as the outer solution. More precisely, we use the result derived in §2 to construct the overall solution in the upper-half domain, which is possible because the temperature of the boundary is uniform. The effect of the discontinuous surface temperature is then transferred to the mismatch of the diffuse reflection conditions (3.2) and (3.3) on $x_1 = \mp\pi/2$ and $x_2 > 0$ and the reflection condition (3.5) on $x_2 = 0$ and $-\pi/2 < x_1 < \pi/2$ at the corners $(x_1, x_2) = (\mp\pi/2, 0)$. This mismatch causes an abrupt spatial variation of the solution in the vicinity of the corner, which Sone's asymptotic solution cannot describe. Thus, we require an internal layer in the vicinity of the corner to alter the Sone's asymptotic solution in a suitable way. The introduction of this new layer (different from the Knudsen layer) is the key ingredient of the present analysis.

In this paper, we shall carry out the asymptotic analysis to the first order of ε .

3.2.1. Outer solution: zeroth order in ε

Let us consider the overall solution in the channel, which is intended to describe the behaviour of the gas except in the region close to the point of the surface temperature discontinuity. This solution is assumed to have the length scale of variation of the order of unity except in a thin layer adjacent to the boundary (the Knudsen layer), where the solution is allowed to change abruptly in the direction normal to the boundary. We call this solution the outer solution and denote it by attaching the subscript F as ϕ_F (or ϕ_F^\pm). In this section, we obtain the zeroth-order (leading-order) approximation of the outer solution ϕ_F^+ .

First, putting aside the potential difficulty which may arise near the discontinuity points, we express ϕ_F^+ as the combination of the Hilbert solution ϕ_H^+ and the Knudsen-layer correction ϕ_K^+ :

$$\phi_F^+ = \phi_H^+ + \phi_K^+. \quad (3.6)$$

The length scale of variation of the Hilbert solution is of the order of unity, whereas the Knudsen-layer correction, which is appreciable only in a thin layer adjacent to the boundary, has the length scale of variation of the order of ε in the direction normal

to the boundary (i.e. $\partial_i \phi_H = O(\phi_H)$, $\partial_1 \phi_K = O(\phi_K/\varepsilon)$ and $\partial_2 \phi_K = O(\phi_K)$). According to § 2, ϕ_H^+ and ϕ_K^+ are expanded in ε as

$$\phi_H^+ = \phi_{H0}^+ + \varepsilon \phi_{H1}^+ + \dots, \tag{3.7a}$$

$$\phi_K^+ = \varepsilon \phi_{K1}^+ + \dots. \tag{3.7b}$$

Thus, substituting the above expansions into (3.6), we obtain the expansion of the outer solution ϕ_F^+ in ε in the form

$$\phi_F^+ = \phi_{F0}^+ + \varepsilon \phi_{F1}^+ + \dots, \tag{3.8}$$

where

$$\phi_{F0}^+ = \phi_{H0}^+, \tag{3.9a}$$

$$\phi_{F1}^+ = \phi_{H1}^+ + \phi_{K1}^+. \tag{3.9b}$$

Corresponding to the expansion of ϕ_F^+ , the macroscopic quantities are also expanded in ε as

$$h_F^+ = h_{F0}^+ + \varepsilon h_{F1}^+ + \dots, \quad (h = \omega, u_i, \tau, P), \tag{3.10}$$

where

$$h_{F0}^+ = h_{H0}^+, \tag{3.11a}$$

$$h_{F1}^+ = h_{H1}^+ + h_{K1}^+. \tag{3.11b}$$

The relation between h_{Hm}^+ and ϕ_{Hm}^+ and that between h_{Km}^+ and ϕ_{Km}^+ are given by (2.8) and (2.38) with $(\phi_{Hm}, h_{Hm}) = (\phi_{Hm}^+, h_{Hm}^+)$ and $(\phi_{Km}, h_{Km}) = (\phi_{Km}^+, h_{Km}^+)$, respectively.

From the result of § 2, the leading-order term of the outer solution ϕ_{F0}^+ is given by the local Maxwellian,

$$\phi_{F0}^+ = \phi_{H0}^+ = P_{H0}^+ + 2\zeta_1 u_{1H0}^+ + 2\zeta_2 u_{2H0}^+ + (\zeta_j^2 - \frac{5}{2}) \tau_{H0}^+, \tag{3.12}$$

where the macroscopic variables solve the following Stokes problem in $D^+ = \{(x_1, x_2) \mid -\pi/2 < x_1 < \pi/2, x_2 > 0\}$:

$$\partial_i P_{H0}^+ = 0, \tag{3.13a}$$

$$\partial_i u_{iH0}^+ = 0, \quad \gamma_1 \nabla^2 u_{iH0}^+ - \partial_i P_{H1}^+ = 0, \tag{3.13b}$$

$$\nabla^2 \tau_{H0}^+ = 0, \tag{3.13c}$$

with the boundary conditions

$$u_{iH0}^+ = 0, \quad \left(x_1 = \mp \frac{\pi}{2}, x_2 > 0\right), \tag{3.14a}$$

$$\tau_{H0}^+ = \tau_w, \quad \left(x_1 = \mp \frac{\pi}{2}, x_2 > 0\right), \tag{3.14b}$$

supplemented by the condition at $x_2 = 0$, i.e.

$$P_{H0}^+ = u_{1H0}^+ = \tau_{H0}^+ = \partial_2 u_{2H0}^+ = 0, \quad \left(-\frac{\pi}{2} < x_1 < \frac{\pi}{2}, x_2 = 0\right) \tag{3.15}$$

(see (3.5)). Here, $i \in \{1, 2\}$ and $\nabla^2 = \partial_1^2 + \partial_2^2$ (the two-dimensional Laplacian). Equations (3.14a) and (3.14b) are the no-slip/no-jump conditions for the flow velocity

and temperature, respectively (see (2.44)). Note that the density is determined from the temperature and pressure by the relation $\omega_{H0}^+ = P_{H0}^+ - \tau_{H0}^+$.

First,

$$P_{H0}^+ = 0 \tag{3.16}$$

trivially satisfies (3.13a) and (3.15). Next, it is readily seen that

$$u_{iH0}^+ = 0, \quad P_{H1}^+ = 0 \tag{3.17}$$

is also a trivial solution to the Stokes equations (3.13b) that satisfies the boundary conditions (3.14a) and (3.15). Note that P_{H1}^+ is only determined up to an additive constant from the Stokes equation. This constant, which should be determined from the information on the higher order, turns out to be zero if one considers the requirement (3.5). This result has already been used in (3.17). On the other hand, τ_{H0}^+ satisfying the Laplace equation (3.13c) and the boundary conditions (3.14b) and (3.15) is given by

$$\tau_{H0}^+ = \frac{\tau_w}{\pi} \text{Arg} \left(\frac{1 + \sin z}{1 - \sin z} \right), \tag{3.18a}$$

$$z = x_1 + i x_2, \tag{3.18b}$$

where i is the imaginary unit. To summarize, the leading-order term of the outer solution is obtained as

$$\phi_{F0}^+ = \left(\zeta_j^2 - \frac{5}{2} \right) \tau_{H0}^+, \tag{3.19}$$

with τ_{H0}^+ given by (3.18).

We observe that τ_{H0}^+ takes different values depending on the way of approach to the point $(x_1, x_2) = (-\pi/2, 0)$ or $(\pi/2, 0)$. This is seen by introducing a local polar coordinate system (r, θ) centred at $(x_1, x_2) = (\mp\pi/2, 0)$ by

$$x_1 = \mp \frac{\pi}{2} \pm r \cos \theta, \quad x_2 = r \sin \theta, \quad \left(\text{near } (x_1, x_2) = \left(\mp \frac{\pi}{2}, 0 \right) \right) \tag{3.20}$$

$(0 \leq \theta \leq \pi/2)$. Expanding τ_{H0}^+ near each of the discontinuity points in terms of small r , we obtain

$$\frac{\tau_{H0}^+}{\tau_w} = \frac{2}{\pi} \theta + \frac{r^2}{6\pi} \sin 2\theta + O(r^4), \quad (r \ll 1). \tag{3.21}$$

This shows that the limiting value of τ_{H0}^+ and therefore that of ϕ_{F0}^+ as $r \searrow 0$ are not uniquely determined but depend on θ .

3.2.2. Outer solution: first order in ε

Next, we proceed to the first order in the expansion of the outer solution. Unlike the zeroth order, ϕ_{F1}^+ is composed of the Hilbert part ϕ_{H1}^+ and the Knudsen-layer part ϕ_{K1}^+ (see (3.9b)). More precisely, with (3.18) and (3.17) obtained above, (2.43) with $\partial_3 = u_{3H1} = 0$ is computed to give

$$\begin{aligned} \phi_{H1}^+ &= 2\zeta_1 u_{1H1}^+ + 2\zeta_2 u_{2H1}^+ + \left(\zeta_j^2 - \frac{5}{2} \right) \tau_{H1}^+ \\ &\quad - \frac{4\tau_w}{\pi} A(\zeta) \frac{\zeta_1 \sin x_1 \sinh x_2 + \zeta_2 \cos x_1 \cosh x_2}{\cos(2x_1) + \cosh(2x_2)}, \end{aligned} \tag{3.22a}$$

$$\phi_{K1}^+ = -\frac{2\tau_w}{\pi} \frac{1}{\sinh x_2} \left(\varphi_1^{(0)}(|x_1 + \pi/2|/\varepsilon, \zeta_1, \zeta) + \varphi_1^{(0)}(|x_1 - \pi/2|/\varepsilon, -\zeta_1, \zeta) \right), \tag{3.22b}$$

where $\zeta = (\zeta_j^2)^{1/2}$ and A and $\varphi_1^{(0)}$ are the functions defined in (2.17a) and (2.32a), respectively. Note that $\varphi_1^{(0)}$ is meaningful only in the Knudsen layer. Therefore, there is no overlap of the two terms in (3.22b). The quantities $u_{iH1}^+ = u_{iH1}^+(x_1, x_2)$ and $\tau_{H1}^+ = \tau_{H1}^+(x_1, x_2)$ contained in (3.22a) are determined by solving the first-order Stokes problem. We will present the explicit form of the problem later (see (3.37)–(3.39)). For the moment, it suffices to mention that, on solving this problem, we simply obtain the following first-order macroscopic quantities with a trivial flow velocity:

$$\tau_{H1}^+ = -\omega_{H1}^+ = -\frac{8\tau_w c_1^{(0)} x_2 \cos x_1 \cosh x_2 + x_1 \sin x_1 \sinh x_2}{\pi^2 \cos(2x_1) + \cosh(2x_2)}, \tag{3.23a}$$

$$u_{1H1}^+ = u_{2H1}^+ = 0, \quad P_{H2}^+ = \text{const.} \tag{3.23b}$$

Note that the trivial flow velocity is the consequence of the no-slip boundary condition $u_{iH1} = 0$ on the boundary, which results from (2.45) because τ_w is constant and $u_{iH0} = 0$.

Of course, our interest is a non-trivial flow velocity and the above result needs to be modified in a suitable way. At this point, however, we simply examine how ϕ_{F1}^+ thus obtained (denoted by ϕ_{F1*}^+) behaves near the points of discontinuity.

Using again the local polar coordinates introduced in (3.20) as well as the corresponding circumferential molecular velocity $\zeta_\theta = \mp \zeta_1 \sin \theta + \zeta_2 \cos \theta$ near $(x_1, x_2) = (\mp \pi/2, 0)$, the essential terms of $\phi_{F1*}^+ = \phi_{H1}^+ + \phi_{K1}^+$ (with (3.22) and (3.23)) in the vicinity of $(x_1, x_2) = (\mp \pi/2, 0)$ takes the form

$$\phi_{F1*}^+ \simeq -\frac{2\tau_w}{\pi} \left[\frac{c_1^{(0)} \sin \theta}{r} \left(\zeta_j^2 - \frac{5}{2} \right) + \frac{\zeta_\theta}{r} A(\zeta) + \frac{1}{x_2} \varphi_1^{(0)}(|x_1 \pm \pi/2|/\varepsilon, \pm \zeta_1, \zeta) \right] + O(r), \quad (r \ll 1). \tag{3.24}$$

Thus, $|\phi_{F1*}^+|$ diverges with the rate r^{-1} on approaching the points of discontinuity. In other words, the outer solution based on Sone’s asymptotic theory is valid only in the region $r \gg \varepsilon$.

3.2.3. Inner solution: zeroth order (leading order) in ε

We have seen that the outer solution breaks down in the vicinity of the point where the surface temperature has a jump. The reason is that the underlying length scale of variation of the Hilbert solution and that of the Knudsen-layer correction are too restrictive to describe the abrupt change that the flow undergoes near the points of discontinuity. This motivates us to introduce another inner layer near $(x_1, x_2) = (\mp \pi/2, 0)$, in which the solution is allowed to vary in x_1 and x_2 on the length scale of variation of the order of the (scaled) mean free path. This localized region near each of the discontinuity points may be called the Knudsen zone (see figure 2). Accordingly, the solution in this region is hereafter denoted by $\phi = \phi_Z$, i.e. $\partial_i \phi_Z = O(\phi_Z/\varepsilon)$.

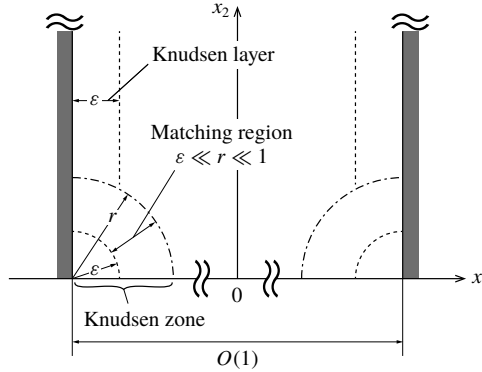


FIGURE 2. Schematics of the solution structure. Only the upper-half domain is shown.

In order to analyse the Knudsen zone, it is convenient to introduce new variables y_i (the inner variables) and ξ_i by the relations

$$\left. \begin{aligned} x_1 &= \mp \frac{\pi}{2} \pm \varepsilon y_1, & x_2 &= \varepsilon y_2, \\ (\xi_1, \xi_2, \xi_3) &= (\pm \zeta_1, \zeta_2, \zeta_3), & \text{near } (x_1, x_2) &= \left(\mp \frac{\pi}{2}, 0 \right), \end{aligned} \right\} \quad (3.25)$$

and express the solution as $\phi_Z = \phi_Z(y_1, y_2, \xi_i)$. If we further expand ϕ_Z in a power series of ε , i.e.

$$\phi_Z = \phi_{Z0} + \varepsilon \phi_{Z1} + \dots, \quad (3.26)$$

the leading-order term ϕ_{Z0} satisfies the following equation and boundary condition:

$$\xi_1 \frac{\partial \phi_{Z0}}{\partial y_1} + \xi_2 \frac{\partial \phi_{Z0}}{\partial y_2} = \mathcal{L}(\phi_{Z0}), \quad (y_1 > 0, \quad -\infty < y_2 < \infty), \quad (3.27)$$

$$\phi_{Z0} = 2\sqrt{\pi} \int_{\xi_1 < 0} |\xi_1| \phi_{Z0} E \, d\xi \pm (\xi_j^2 - 2)\tau_w, \quad \xi_1 > 0, \quad (y_1 = 0, \quad \pm y_2 > 0), \quad (3.28)$$

where $E = E(\xi_i)$ and $d\xi = d\xi_1 d\xi_2 d\xi_3$.

To derive the boundary condition at infinity, we use the asymptotic matching. Let us consider a point (x_1, x_2) close to the discontinuity point that satisfies $r = \sqrt{(x_1 \pm \pi/2)^2 + x_2^2} \ll 1$ and $r \gg \varepsilon$. As discussed above, the outer solution is valid in the region $r \gg \varepsilon$. If we further assume that the inner solution is valid in the region $r \ll 1$, there appears a cross-over of the two solutions in the region $\varepsilon \ll r \ll 1$. With this kept in mind, we express the zeroth-order outer solution $\phi_{F0} = \phi_{F0}(x_1, x_2, \zeta_i)$ in terms of the inner variables (y_1, y_2, ξ_i) . As the result, we obtain the following asymptotic expression of the outer solution $\phi_F = \phi_{F0} + \varepsilon \phi_{F1} + \dots$ in terms of ε in the vicinity of $(x_1, x_2) = (\mp \pi/2, 0)$:

$$\phi_F^\dagger = \frac{2\tau_w}{\pi} \left(\xi_j^2 - \frac{5}{2} \right) \theta + O(\varepsilon), \quad (\text{as } \varepsilon \searrow 0 \text{ with } r = \varepsilon \tilde{r} \text{ fixed}), \quad (3.29)$$

where $\theta = \text{Arctan}(y_2/y_1)$, $\tilde{r} = \sqrt{y_1^2 + y_2^2}$ and the superscript \dagger is attached to emphasize that the outer solution is expressed in terms of the inner variables. Note that the first

term is independent of \tilde{r} , because so is the first term of (3.21), but the $O(\varepsilon)$ term is generally \tilde{r} -dependent. Therefore, in order for the inner solution ϕ_Z to match ϕ_F disregarding the error of $O(\varepsilon)$ as $\varepsilon \searrow 0$, we require

$$\phi_{Z0} \rightarrow \frac{2\tau_w}{\pi} \left(\xi_j^2 - \frac{5}{2} \right) \theta, \quad (\tilde{r} \rightarrow \infty). \tag{3.30}$$

Finally, the macroscopic quantities in the Knudsen zone (at the zeroth order) are expressed in terms of ϕ_{Z0} as follows:

$$\omega_{Z0} = \int \phi_{Z0} E d\xi, \quad u_{iZ0} = \int \xi_i \phi_{Z0} E d\xi, \quad (i = 1, 2), \quad u_{3Z0} = 0, \tag{3.31a}$$

$$\tau_{Z0} = \frac{2}{3} \int \left(\xi_j^2 - \frac{3}{2} \right) \phi_{Z0} E d\xi, \quad P_{Z0} = \omega_{Z0} + \tau_{Z0}, \tag{3.31b}$$

where the integration is carried out over the whole ξ_i space.

Equations (3.27), (3.28), and (3.30) form a (spatially two-dimensional) boundary-value problem of the linearized Boltzmann equation for ϕ_{Z0} in a half-space. Physically, the problem describes the steady motion of a rarefied gas caused by a discontinuous surface temperature over a plane boundary in the situation where there is a steady heat flow (flowing in the clockwise direction when $\tau_w > 0$) at a far distance. As we will see, this problem admits a solution with non-zero flow velocity whose magnitude is inversely proportional to the distance from the origin in the far field. From this behaviour at far field, a condition for u_{iH1} of the Hilbert solution is derived.

We may assume that the solution is antisymmetric with respect to (y_2, ξ_2) , i.e.

$$\phi_{Z0}(y_1, -y_2, \xi_1, -\xi_2, \xi_3) = -\phi_{Z0}(y_1, y_2, \xi_1, \xi_2, \xi_3). \tag{3.32}$$

Therefore, we only need to solve the problem in the upper-half domain $y_2 > 0$, by imposing the reflection condition at $y_2 = 0$, i.e.

$$\phi_{Z0}(y_1, 0, \xi_1, -\xi_2, \xi_3) = -\phi_{Z0}(y_1, 0, \xi_1, \xi_2, \xi_3), \quad \xi_2 > 0. \tag{3.33}$$

3.2.4. Far-field behaviour of the gas in the Knudsen zone

This subsection is devoted to a discussion of the asymptotic behaviour of the solution in the far field ($\tilde{r} = \sqrt{y_1^2 + y_2^2} \gg 1$) of the Knudsen-zone problem. The key observation is that, in the far field, the length scale of variation of the solution is large (i.e. the local Knudsen number is small), and one can apply Sone's asymptotic method (the linear theory (Sone 2007, chap. 3)). The application of the theory is straightforward and the derivation is outlined in appendix A. Here, we list the resulting asymptotic forms of the macroscopic quantities as well as that of the velocity distribution function in the far region $\tilde{r} \gg 1$.

(a) Macroscopic quantities

$$\begin{aligned} \frac{u_{rZ0}}{\tau_w} = & \frac{\Gamma_Z^{(1)}}{\tilde{r}} \sin 2\theta - \frac{3\Gamma_Z^{(2)}(\sin 3\theta + \sin \theta) - 2 \left(\Gamma_Z^{(1)} b_1^{(1)} + \frac{c_1^{(0)} b_2^{(1)} + b_3^{(1)}}{\pi} \right) \sin \theta}{\tilde{r}^2} \\ & + \frac{2}{y_2^2} \left(\Gamma_Z^{(1)} Y_1^{(1)}(y_1) + \frac{c_1^{(0)} Y_2^{(1)}(y_1) + Y_3^{(1)}(y_1)}{\pi} \right) \sin \theta + \dots, \end{aligned} \tag{3.34a}$$

$$\frac{u_{\theta Z0}}{\tau_w} = \frac{\Gamma_Z^{(2)}(\cos 3\theta + 3 \cos \theta) - 2 \left(\Gamma_Z^{(1)} b_1^{(1)} + \frac{c_1^{(0)} b_2^{(1)} + b_3^{(1)}}{\pi} \right) \cos \theta}{\tilde{r}^2} + \frac{2}{y_2^2} \left(\Gamma_Z^{(1)} Y_1^{(1)}(y_1) + \frac{c_1^{(0)} Y_2^{(1)}(y_1) + Y_3^{(1)}(y_1)}{\pi} \right) \cos \theta + \dots, \tag{3.34b}$$

$$\frac{P_{Z0}}{\tau_w} = -\frac{2}{\pi} \frac{1}{y_2} \left(\Omega_1^{(0)}(y_1) + \Theta_1^{(0)}(y_1) \right) + \frac{2\gamma_1 \Gamma_Z^{(1)}}{\tilde{r}^2} \sin 2\theta + \dots, \tag{3.34c}$$

$$\frac{\tau_{Z0}}{\tau_w} = \frac{2}{\pi} \theta - \frac{2}{\pi} \left(\frac{c_1^{(0)}}{\tilde{r}} \sin \theta + \frac{1}{y_2} \Theta_1^{(0)}(y_1) \right) + \frac{\Lambda_Z^{(2)}}{\tilde{r}^2} \sin 2\theta + \dots, \tag{3.34d}$$

$$\frac{\omega_{Z0}}{\tau_w} = -\frac{2}{\pi} \theta + \frac{2}{\pi} \left(\frac{c_1^{(0)}}{\tilde{r}} \sin \theta - \frac{1}{y_2} \Omega_1^{(0)}(y_1) \right) + \frac{2\gamma_1 \Gamma_Z^{(1)} - \Lambda_Z^{(2)}}{\tilde{r}^2} \sin 2\theta + \dots. \tag{3.34e}$$

(b) Velocity distribution function

$$\begin{aligned} \frac{\phi_{Z0}}{\tau_w} = & \frac{2\Gamma_Z^{(1)}}{\tilde{r}} \xi_r \sin 2\theta + \frac{2}{\pi} \left(\xi_j^2 - \frac{5}{2} \right) \left(\theta - \frac{c_1^{(0)}}{\tilde{r}} \sin \theta + \frac{\pi}{2} \frac{\Lambda_Z^{(2)}}{\tilde{r}^2} \sin 2\theta \right) \\ & - \frac{2}{\pi} \left(\frac{\xi_\theta}{\tilde{r}} A(\xi) + \frac{1}{y_2} \varphi_1^{(0)}(y_1, \xi_1, \xi) \right) + \frac{2\gamma_1 \Gamma_Z^{(1)}}{\tilde{r}^2} \sin 2\theta \\ & - 2\Gamma_Z^{(2)} \frac{3\xi_r(\sin 3\theta + \sin \theta) - \xi_\theta(\cos 3\theta + 3 \cos \theta)}{\tilde{r}^2} \\ & + 4 \left(\Gamma_Z^{(1)} b_1^{(1)} + \frac{c_1^{(0)} b_2^{(1)} + b_3^{(1)}}{\pi} \right) \frac{\xi_r \sin \theta - \xi_\theta \cos \theta}{\tilde{r}^2} \\ & + \Gamma_Z^{(1)} \left(\frac{(\xi_r^2 - \xi_\theta^2) \sin 2\theta - 2\xi_r \xi_\theta \cos 2\theta}{\tilde{r}^2} B(\xi) + \frac{2\xi_2}{y_2^2} \varphi_1^{(1)}(y_1, \xi_1, \xi) \right) \\ & + \frac{2}{\pi} c_1^{(0)} \left(-\frac{\xi_r \sin \theta - \xi_\theta \cos \theta}{\tilde{r}^2} A(\xi) + \frac{\xi_2}{y_2^2} \varphi_2^{(1)}(y_1, \xi_1, \xi) \right) \\ & + \frac{2}{\pi} \left(\frac{2\xi_r \xi_\theta}{\tilde{r}^2} F(\xi) + \frac{\xi_2}{y_2^2} \varphi_3^{(1)}(y_1, \xi_1, \xi) \right) + \dots. \end{aligned} \tag{3.35}$$

Here, $\Gamma_Z^{(1)}$, $\Gamma_Z^{(2)}$ and $\Lambda_Z^{(2)}$ are constants which should be determined together with the solution, $\xi = (\xi_r^2 + \xi_\theta^2 + \xi_3^2)^{1/2}$,

$$\begin{pmatrix} \xi_r & u_{rZ0} \\ \xi_\theta & u_{\theta Z0} \end{pmatrix} = \begin{pmatrix} \cos \theta & \sin \theta \\ -\sin \theta & \cos \theta \end{pmatrix} \begin{pmatrix} \xi_1 & u_{1Z0} \\ \xi_2 & u_{2Z0} \end{pmatrix}, \tag{3.36}$$

and the constants $(\gamma_1, c_1^{(0)}, b_j^{(1)})$ and the functions $(A, B, \varphi_1^{(0)}, \varphi_j^{(1)}, \Omega_1^{(0)}, \Theta_1^{(0)}, Y_j^{(1)})$ are the same as those introduced in § 2 (see tables 1 and 2).

As seen from (3.34), the flow velocity has radially diverging or converging streamlines depending on $y_1 \geq 0$ in the far field, provided that $\Gamma_Z^{(1)}$ is positive. Our preliminary numerical analysis employing the BGK model shows that this is likely to hold, which is also consistent with the numerical results shown later in § 4.

The Knudsen-zone problem is spatially two-dimensional, and the numerical analysis is much more difficult than the conventional Knudsen-layer problem, which is spatially one-dimensional. Therefore, we shall present the numerical result of the Knudsen-zone problem in detail in a separate paper. For the moment, we assume that $\Gamma_Z^{(1)}$, $\Gamma_Z^{(2)}$ and $\Lambda_Z^{(2)}$ are known and proceed to the next step of the asymptotic analysis.

3.2.5. Outer solution: first order in ε and a diverging singularity to drive the flow

We go back to the first-order outer solution and consider ϕ_{F1}^+ . Applying the results of §2, the overall behaviour of the macroscopic quantities in the outer region are described by the following Stokes problem:

(a) Equations

$$\partial_i u_{iH1}^+ = 0, \quad \gamma_1 \nabla^2 u_{iH1}^+ - \partial_i P_{H2}^+ = 0, \tag{3.37a}$$

$$\nabla^2 \tau_{H1}^+ = 0. \tag{3.37b}$$

(b) Boundary conditions

$$u_{iH1}^+ = 0, \quad \left(x_1 = \mp \frac{\pi}{2}, \quad x_2 > 0 \right), \tag{3.38a}$$

$$\tau_{H1}^+ = \pm c_1^{(0)} \partial_1 \tau_{H0}^+ = -\frac{2\tau_w c_1^{(0)}}{\pi} \frac{1}{\sinh x_2}, \quad \left(x_1 = \mp \frac{\pi}{2}, \quad x_2 > 0 \right). \tag{3.38b}$$

The conditions (3.38a) and (3.38b) correspond to the no-slip condition for the flow velocity u_{iH1}^+ and to the jump condition for the temperature τ_{H1}^+ , respectively (see (2.45)). Note that there is no thermal slip because τ_{H0}^+ is constant along the boundary $x_1 = \mp \pi/2$. In addition, we impose the following condition at $x_2 = 0$:

$$u_{1H1}^+ = \tau_{H1}^+ = \partial_2 u_{2H1}^+ = 0, \quad \left(-\frac{\pi}{2} < x_1 < \frac{\pi}{2}, \quad x_2 = 0 \right). \tag{3.39}$$

The first order density is obtained from the temperature by $\omega_{H1}^+ = -\tau_{H1}^+$ since $P_{H1}^+ = 0$.

Solving the problem for τ_{H1}^+ , we obtain the temperature τ_{H1}^+ given in (3.23a). On the other hand, equations (3.37a) with (3.38a) and (3.39) yields merely a trivial flow field (3.23b), which is outwith our interest. However, the difference from §3.2.2 is that we have now the Knudsen zone as a part of the solution; a condition for non-trivial flow is obtained by the consideration that the outer solution should match asymptotically the inner solution in the cross-over region.

With the same notation as in (3.20), let us consider a point close to $(x_1, x_2) = (\mp \pi/2, 0)$ for which $\varepsilon \ll r \ll 1$. Note that this range corresponds to $1 \ll \tilde{r} \ll \varepsilon^{-1}$ in the inner region. Therefore, for the corresponding inner solution, we can use the far-field asymptotic form (3.35) for the leading-order Knudsen-zone solution ϕ_{Z0} . With the aid of the relation between the inner and outer variables (i.e. (3.25)), this is further transformed into the expansion in ε as follows:

$$\begin{aligned}
 \frac{\phi_{Z0}^\dagger}{\tau_w} &= \varepsilon \frac{2\Gamma_Z^{(1)}}{r} \zeta_r \sin 2\theta + \frac{2}{\pi} \left(\zeta_j^2 - \frac{5}{2} \right) \left(\theta - \varepsilon \frac{c_1^{(0)}}{r} \sin \theta \right) \\
 &\quad - \varepsilon \frac{2}{\pi} \left(\frac{\zeta_\theta}{r} A(\zeta) + \frac{1}{x_2} \varphi_1^{(0)} (|x_1 \pm \pi/2| / \varepsilon, \pm \zeta_1, \zeta) \right) + O(\varepsilon^2) \\
 &= \frac{2}{\pi} \left(\zeta_j^2 - \frac{5}{2} \right) \theta + \varepsilon \left[\frac{2\Gamma_Z^{(1)}}{r} \zeta_r \sin 2\theta - \frac{2}{\pi} \frac{c_1^{(0)}}{r} \sin \theta \left(\zeta_j^2 - \frac{5}{2} \right) \right. \\
 &\quad \left. - \frac{2}{\pi} \frac{\zeta_\theta}{r} A(\zeta) - \frac{2}{\pi} \frac{1}{x_2} \varphi_1^{(0)} (|x_1 \pm \pi/2| / \varepsilon, \pm \zeta_1, \zeta) \right] \\
 &\quad + O(\varepsilon^2), \quad \text{as } \varepsilon \searrow 0 \text{ with } \tilde{r} = \frac{r}{\varepsilon} \text{ fixed,} \tag{3.40}
 \end{aligned}$$

where the superscript † is attached to indicate that the function is expressed in terms of the outer variables (x_i, ζ_i) . On the other hand, equations (3.19), (3.22a) with (3.23a), and (3.22b) give, for small r ,

$$\begin{aligned}
 \phi_F^+ &= \phi_{F0}^+ + \varepsilon \phi_{F1}^+ + \dots \\
 &= \frac{2\tau_w}{\pi} \left(\zeta_j^2 - \frac{5}{2} \right) (\theta + O(r^2)) \\
 &\quad + \varepsilon \left[2(\zeta_r u_{rH1}^+ + \zeta_\theta u_{\theta H1}^+) - \frac{2\tau_w}{\pi} \frac{c_1^{(0)}}{r} \sin \theta \left(\zeta_j^2 - \frac{5}{2} \right) \right. \\
 &\quad \left. - \frac{2\tau_w}{\pi} \frac{\zeta_\theta}{r} A(\zeta) - \frac{2\tau_w}{\pi} \frac{1}{x_2} \varphi_1^{(0)} (|x_1 \pm \pi/2| / \varepsilon, \pm \zeta_1, \zeta) + O(r) \right] + \dots \tag{3.41}
 \end{aligned}$$

Therefore, the comparison of the ε -order terms in the two expressions shows that the macroscopic flow velocity u_{rH1}^+ and $u_{\theta H1}^+$ appearing in (3.41) must satisfy the following matching conditions as $r \searrow 0$:

$$u_{rH1}^+ \rightarrow \frac{\tau_w \Gamma_Z^{(1)}}{r} \sin 2\theta, \quad u_{\theta H1}^+ \rightarrow 0, \quad (r \rightarrow 0). \tag{3.42}$$

The condition (3.42) plays the role of a driving force for the flow caused by a discontinuous surface temperature on a planar surface, and its magnitude $\Gamma_Z^{(1)}$ is determined through the analysis of the Knudsen-zone problem (or two-dimensional Knudsen-layer problem). In summary, the flow field at the first order in ε is determined by solving the Stokes equation (3.37a) under the boundary conditions (3.38a), (3.39) and the matching condition (3.42).

3.3. Summary of the fluid-dynamic-type system

We summarize the result of the asymptotic analysis carried out in this section. Outside the Knudsen zone near the discontinuity point, the macroscopic variables are expressed as

$$u_i = \varepsilon u_{iH1} + O(\varepsilon^2), \quad P = \varepsilon P_{K1} + O(\varepsilon^2), \tag{3.43a}$$

$$\tau = \tau_{H0} + \varepsilon(\tau_{H1} + \tau_{K1}) + O(\varepsilon^2), \tag{3.43b}$$

$$\omega = \omega_{H0} + \varepsilon(\omega_{H1} + \omega_{K1}) + O(\varepsilon^2), \tag{3.43c}$$

where τ_{H0} is given by (3.18), and τ_{H1} and u_{iH1} ($u_{3H1} = 0$) are determined by solving the following Stokes problem:

(a) Equations

$$\partial_i u_{iH1} = 0, \quad \gamma_1 \nabla^2 u_{iH1} - \partial_i P_{H2} = 0, \tag{3.44a}$$

$$\nabla^2 \tau_{H1} = 0. \tag{3.44b}$$

(b) Boundary conditions

$$u_{iH1} = 0, \quad \left(x_1 = \mp \frac{\pi}{2}, x_2 \neq 0\right), \tag{3.45a}$$

$$\tau_{H1} = \pm c_1^{(0)} \partial_1 \tau_{H0}, \quad \left(x_1 = \mp \frac{\pi}{2}, x_2 \neq 0\right). \tag{3.45b}$$

(c) Matching conditions

$$u_{rH1} \rightarrow \frac{\tau_w \Gamma_Z^{(1)}}{r} \sin 2\theta, \quad u_{\theta H1} \rightarrow 0, \quad (x_1, x_2) \rightarrow \left(\mp \frac{\pi}{2}, 0\right). \tag{3.46}$$

Here, (r, θ) ($-\pi/2 \leq \theta \leq \pi/2$) is the polar coordinate system centred at $(x_1, x_2) = (\mp\pi/2, 0)$, i.e. $x_1 = \mp\pi/2 \pm r \cos \theta$ and $x_2 = r \sin \theta$. The density ω up to the first order in ε is related to the temperature as $\omega_{H0} = -\tau_{H0}$ and $\omega_{H1} = -\tau_{H1}$ since $P_H = O(\varepsilon^2)$.

In this paper, we will not give the solution to the above problem for u_{iH1} and P_{H2} (τ_{H1} and ω_{H1} are given in (3.23a)). Instead, we verify whether the diverging condition (3.46) is actually observed around a flat boundary with a discontinuous surface temperature in a direct numerical computation.

We close this section with the following comments. In this study, we used the linearized Boltzmann equation. The linearization is legitimate as long as the jump $2T_0|\tau_w|$ in the surface temperature is sufficiently small compared with the reference temperature T_0 . There is no restriction imposed on the magnitude of the gradient of ϕ . In fact, it becomes very large near the point of discontinuity. On the other hand, the Hilbert solution, which is described by the Stokes system shown above, is subject to the restriction that the order of magnitude of the spatial derivative should not exceed that of the solution itself (see the sentence following (3.6)). Clearly, this cannot be satisfied uniformly in space due to the condition (3.46). Accordingly, it should be understood that the Stokes system describes the Hilbert solution except in the vicinity of the discontinuity point, although it is solved in the entire domain. It should also be noted that this type of singular condition is often used in conjunction with fluid equations in fluid mechanics. Indeed, the condition (3.46) has the same singularity as the (linearized) Jeffery–Hamel flow with a source-sink pair in the case where the opening angle between two intersecting planes is π (thus, forming a plane). In this sense, the present analysis also sheds light on the interpretation of the diverging singularity frequently encountered in fluid mechanics.

4. Numerical analysis of a flow driven by a discontinuous surface temperature

In this section, we carry out a numerical analysis to confirm the results of the present analysis, in particular, the macroscopic behaviour near the points of discontinuity. The problem we solve is the following.

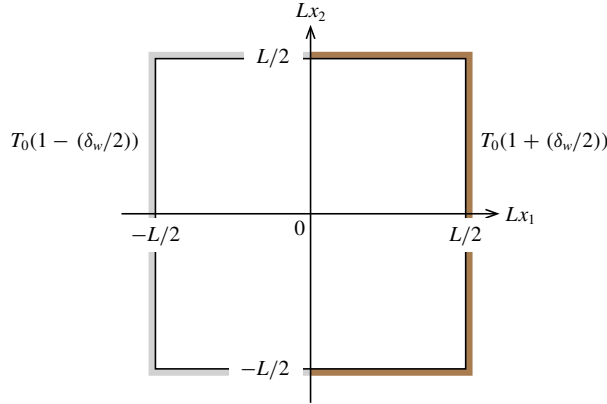


FIGURE 3. A two-dimensional square vessel with a discontinuous surface temperature distribution.

Let L and T_0 be the characteristic length and temperature, respectively. Consider a rarefied gas confined in a two-dimensional square vessel with width L (see figure 3). Let us denote by Lx_i the space rectangular coordinate system. Then, the walls of the vessel, which are supposed to be at rest, are given by the segments $\{x_1 = \pm 1/2, -1/2 \leq x_2 \leq 1/2\}$ and $\{-1/2 \leq x_1 \leq 1/2, x_2 = \pm 1/2\}$. The right-half part $x_1 > 0$ of the vessel is kept at a uniform temperature $T_0(1 + \delta_w/2)$, while the left-half part $x_1 < 0$ is kept at another uniform temperature $T_0(1 - \delta_w/2)$, where δ_w is a positive constant. Thus, the surface temperature distribution along the wall is discontinuous at $(x_1, x_2) = (0, \pm 1/2)$ with jump $T_0\delta_w$. Let ρ_0 and $p_0 = \rho_0RT_0$ be the reference density and pressure, respectively. Investigate the steady behaviour of the gas caused by the discontinuous surface temperature based on the BGK model of the Boltzmann equation and the diffuse reflection boundary condition, under the assumption that δ_w is so small that the equations and boundary conditions can be linearized around the reference equilibrium state at rest with temperature T_0 and density ρ_0 (or pressure p_0).

For the BGK model, the mean free path of the gas molecules in the reference equilibrium state at rest is given by $\ell_0 = (2/\sqrt{\pi})(2RT_0)^{1/2}/(A_c\rho_0)$ with A_c being a positive constant such that $A_c\rho_0$ is the collision frequency in the reference state. Accordingly, the Knudsen number is defined by $Kn = \ell_0/L$, and, as in the foregoing analysis, we mainly use parameter $\varepsilon = (\sqrt{\pi}/2)Kn$ to specify the degree of gas rarefaction. Let us denote by $(2RT_0)^{1/2}\zeta_i$ the molecular velocity, by $\rho_0(2RT_0)^{-3/2}(1 + \phi(x_1, x_2, \zeta_i))E$ the velocity distribution function, by $\rho_0(1 + \omega(x_1, x_2))$ the density, by $(2RT_0)^{1/2}u_i(x_1, x_2)$ the flow velocity ($u_3 = 0$) and by $T_0(1 + \tau(x_1, x_2))$ the temperature. Then, the linearized BGK equation in the present steady two-dimensional problem is written as

$$\zeta_1 \partial_1 \phi + \zeta_2 \partial_2 \phi = \frac{1}{\varepsilon} \left(-\phi + \omega + 2\zeta_1 u_1 + 2\zeta_2 u_2 + \left(\zeta_j^2 - \frac{3}{2} \right) \tau \right), \tag{4.1a}$$

$$\omega = \langle \phi \rangle, \quad u_i = \langle \zeta_i \phi \rangle, \quad (i = 1, 2), \quad \tau = \frac{2}{3} \left\langle \left(\zeta_j^2 - \frac{3}{2} \right) \phi \right\rangle. \tag{4.1b}$$

The boundary conditions are summarized as

$$\phi = -2\sqrt{\pi} \int_{\zeta_n < 0} \zeta_n \phi E d\zeta - \frac{\delta_w}{2} (\zeta_j^2 - 2), \quad \text{for } \zeta_n > 0, \\ \left(-\frac{1}{2} < x_1 < 0, \quad x_2 = \pm \frac{1}{2}\right) \quad \text{or} \quad \left(x_1 = -\frac{1}{2}, \quad -\frac{1}{2} < x_2 < \frac{1}{2}\right), \quad (4.2a)$$

$$\phi = -2\sqrt{\pi} \int_{\zeta_n < 0} \zeta_n \phi E d\zeta + \frac{\delta_w}{2} (\zeta_j^2 - 2), \quad \text{for } \zeta_n > 0, \\ \left(0 < x_1 < \frac{1}{2}, \quad x_2 = \pm \frac{1}{2}\right) \quad \text{or} \quad \left(x_1 = \frac{1}{2}, \quad -\frac{1}{2} < x_2 < \frac{1}{2}\right), \quad (4.2b)$$

where $\zeta_n = \zeta_i n_i$ and n_i is the unit normal vector on the boundary pointed to the gas, i.e.

$$n_i = \begin{cases} (0, \mp 1, 0) & (-\frac{1}{2} < x_1 < \frac{1}{2}, \quad x_2 = \pm \frac{1}{2}), \\ (\pm 1, 0, 0) & (x_1 = \mp \frac{1}{2}, \quad -\frac{1}{2} < x_2 < \frac{1}{2}). \end{cases} \quad (4.3)$$

Apart from the linearization, the problem is the same as the one investigated in Aoki *et al.* (2001), where the nonlinear BGK equation was solved numerically (under the diffuse reflection without linearization). Since the linearization is not essential for the numerical treatment, we adopted the same numerical method here. It is a hybrid method combining the finite-difference method and the method of characteristics and is designed to capture the propagation of the discontinuity in the phase space. See Aoki *et al.* (2001) for further details of the numerical method.

We may assume that the solution ϕ is symmetric with respect to the x_1 axis and antisymmetric with respect to the x_2 axis, namely,

$$\phi(-x_1, x_2, -\zeta_1, \zeta_2, \zeta_3) = \phi(x_1, x_2, \zeta_1, \zeta_2, \zeta_3), \quad (4.4a)$$

$$\phi(x_1, -x_2, \zeta_1, -\zeta_2, \zeta_3) = -\phi(x_1, x_2, \zeta_1, \zeta_2, \zeta_3). \quad (4.4b)$$

Therefore, the computation was carried out only in the quadrant $0 \leq x_1 \leq 1/2$ and $-1/2 \leq x_2 \leq 0$.

For the numerical computation, the domain $\{(x_1, x_2) \mid 0 \leq x_1 \leq 1/2, \quad -1/2 \leq x_2 \leq 0\}$ was subdivided into 320×320 (160×160) non-uniform rectangular meshes for $\varepsilon \leq 0.01$ ($\varepsilon > 0.01$). For the molecular velocity, 75×2045 ($\zeta_r \times \theta_\zeta$) non-uniform grids were used, where (ζ_r, θ_ζ) are the polar coordinates for (ζ_1, ζ_2) , i.e. $\zeta_1 = \zeta_r \cos \theta_\zeta$ and $\zeta_2 = \zeta_r \sin \theta_\zeta$.

In figure 4, we show the flow velocity (u_1, u_2) and temperature τ in the case of $\varepsilon = 0.01$. A fairly noticeable flow is induced near the point of discontinuity, which drives the overall flow in the container. Near the point of discontinuity, the isolines of the temperature are concentrated, implying that a strong temperature gradient in the clockwise direction is formed near the point. It is interesting to note that these features bear resemblance to the flow around a sharp edge (Taguchi & Aoki 2012).

To have a closer look at the flow structure, we investigate the magnitude of the flow velocity $|u_i| = (u_1^2 + u_2^2)^{1/2}$ in two different ways. In the panel (a) of figure 5, we plot the variations of the flow speed $|u_i|$ in terms of ε at five locations in the domain, i.e. $(x_1, x_2) = (0.005, -0.495), (0.02, -0.495), (0.05, -0.495), (0.3, -0.4)$ and $(0, -0.275)$. It is seen from the figure that, with the decrease of ε from 1 to 0.002, the flow speed increases first, attains the local maximum and then decreases. Moreover, judging from the slope of the double-log plot, its decay rate for $\varepsilon \ll 1$

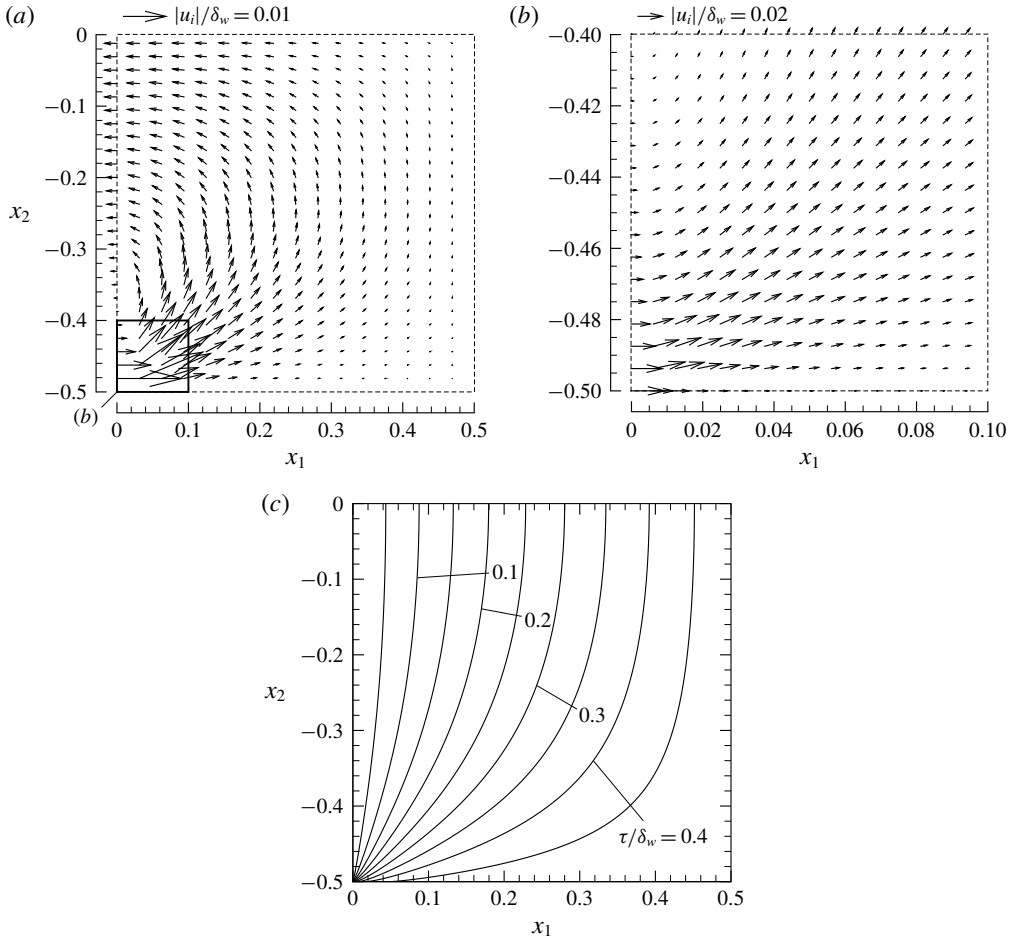


FIGURE 4. The flow velocity (u_1, u_2) and temperature τ in the case of $\epsilon = 0.01$. In panels (a) and (b), the arrow indicates the flow velocity vector $\delta_w^{-1}(u_1, u_2)$ at its starting point. The length corresponding to the magnitude $\delta_w^{-1}|u_i| = \delta_w^{-1}(u_1^2 + u_2^2)^{1/2} = 0.01$ in panel (a) or 0.02 in panel (b) is shown on the top of each panel. Note that the vectors are not shown along $x_2 = -0.5$ in panel (a). In panel (c), the isothermal lines $\tau/\tau_w = 0.05m$ ($m = 0, \dots, 9$) are shown.

is likely to be proportional to ϵ , except in the case $(x_1, x_2) = (0.005, -0.495)$ (o). This decaying trend for small ϵ is consistent with our result $u_{iH} = O(\epsilon)$ obtained in the analysis of § 3 (see (3.43)). The case $(x_1, x_2) = (0.005, -0.495)$ exhibits a slower decay rate, but we expect that the plot will also start to follow the same tendency if ϵ is further reduced.

In § 3, we introduced a boundary layer (the Knudsen zone) in the vicinity of the point of discontinuity with the size of the order of ϵ , where the flow velocity should be $|u_i|/\delta_w = O(1)$. To observe the formation of such a boundary-layer structure in the present problem, we plot the flow speed $|u_i|$ at the point $(x_1, x_2) = (a\epsilon \cos \theta, -1/2 + a\epsilon \sin \theta)$ for various values of ϵ , for a given set of $a > 0$ and $\theta \in [0, \pi/2]$. The result is shown in panel (b) of figure 5. The figure shows a clear tendency that $|u_i|$ approaches a non-zero limiting value as ϵ becomes smaller. Note that the point at which $|u_i|$

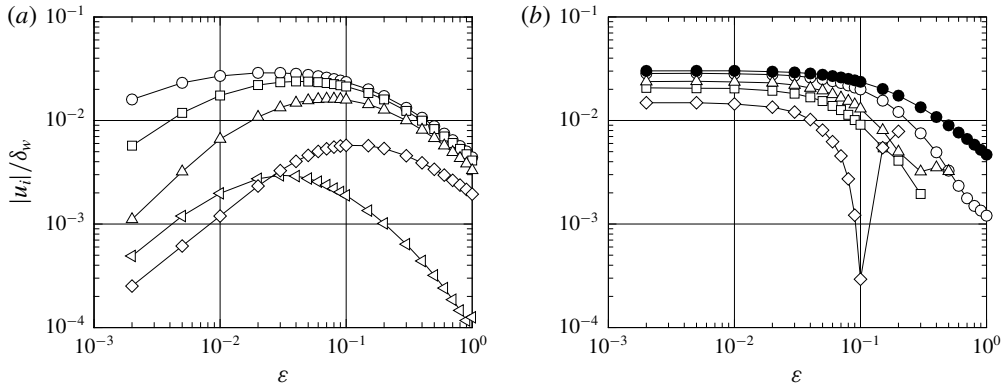


FIGURE 5. The flow speed $|u_i| = (u_1^2 + u_2^2)^{1/2}$ as a function of ε at various points. (a) Graph of $|u_i|$ versus ε at a fixed point in the domain, where $\circ (x_1, x_2) = (0.005, -0.495)$, $\square (0.02, -0.495)$, $\triangle (0.05, -0.495)$, $\diamond (0.3, -0.4)$, $\triangleleft (0, -0.275)$. (b) Graph of $|u_i|$ versus ε at the points $(x_1(\varepsilon), x_2(\varepsilon)) = (a\varepsilon \cos \theta, -1/2 + a\varepsilon \sin \theta)$, where $\circ (a, \theta) = (1/2, \pi/4)$, $\square (2, \pi/4)$, $\triangle (1, \pi/3)$, $\diamond (2, \pi/2)$. The symbol \bullet represents $\sup |u_i|$ in the domain. The numerical results are shown by the symbols, which are connected by the solid lines.

is measured approaches the point of discontinuity, but its relative position remains the same in the scale of ε , or, in other words, in the scale of the mean free path. This implies that there is a kinetic boundary-layer structure in the vicinity of the discontinuity point, which extends over the distance of the order of ε (or the mean free path).

We mention that essentially the same features were already pointed out in Aoki *et al.* (2001), where the nonlinear equations were solved. Indeed, figure 5 corresponds to figure 13 of Aoki *et al.* (2001). The detailed information provided in that reference served as a basic guideline for the present analysis.

We now turn our attention to the validity of the asymptotic expressions (3.21) and (3.46) for the temperature and the flow velocity. For the present problem, they are expressed as

$$\frac{\tau}{\delta_w} \sim \frac{1}{2} - \frac{\theta}{\pi}, \quad \frac{u_r}{\delta_w} \sim \frac{\varepsilon}{r} \sin 2\theta, \quad \text{as } r \searrow 0 \text{ and } \varepsilon \searrow 0 \text{ with } \frac{\varepsilon}{r} = o(1), \quad (4.5)$$

where $u_r = u_1 \cos \theta + u_2 \sin \theta$ is the radial component of the flow velocity around $(x_1, x_2) = (0, -1/2)$ and (r, θ) is the local polar coordinate centred at the point of discontinuity, $(x_1, x_2) = (r \cos \theta, -1/2 + r \sin \theta)$. Note that the expression should hold, theoretically, in the region $\varepsilon \ll r \ll 1$.

Let us first consider the temperature τ . We show in figure 6 the plot of $(\tau/\delta_w)(1/2 - \theta/\pi)^{-1}$ at $(x_1, x_2) = (a\varepsilon^\alpha \cos \theta, -1/2 + a\varepsilon^\alpha \sin \theta)$ for various ε in the cases of $(\alpha, a) = (1/2, 3)$ in panel (a) and $(\alpha, a) = (1/3, 3/2)$ in panel (b). Each panel contains the results for three different values of θ ($\theta = \pi/6, \pi/4, \pi/3$) for comparison. Although it is difficult to draw a decisive conclusion, $(\tau/\delta_w)(1/2 - \theta/\pi)^{-1}$ is seen to approach the limiting value ($=1$) with the decrease of ε irrespective of the values of θ . This supports the asymptotic behaviour shown in (4.5).

Finally, we consider the radial component of the flow velocity u_r . In figure 7, we plot $\delta_w^{-1} a |u_r| / \sin 2\theta$ at $(x_1, x_2) = (a\varepsilon^\alpha \cos \theta, -1/2 + a\varepsilon^\alpha \sin \theta)$ for various ε in the

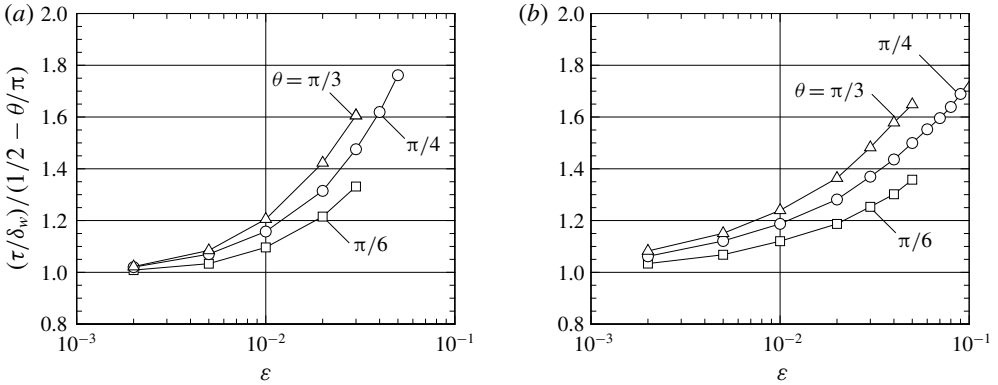


FIGURE 6. The normalized temperature $(\tau/\delta_w)/(1/2 - \theta/\pi)$ at the point $(x_1, x_2) = (a\epsilon^\alpha \cos \theta, -1/2 + a\epsilon^\alpha \sin \theta)$ for various ϵ . (a) $(\alpha, a) = (1/2, 3)$, (b) $(\alpha, a) = (1/3, 3/2)$. The symbols represent the numerical results, which are connected by the solid lines.

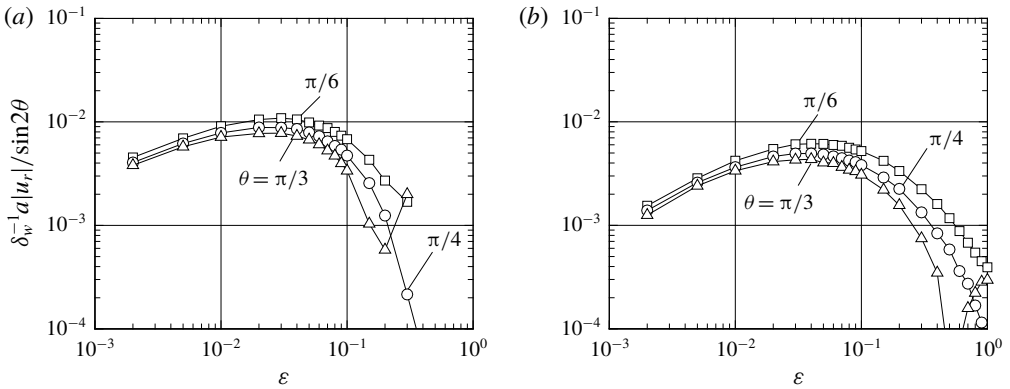


FIGURE 7. The normalized radial flow velocity $\delta_w^{-1}a|u_r|/\sin 2\theta$ at the point $(x_1(\epsilon), x_2(\epsilon)) = (a\epsilon^\alpha \cos \theta, -1/2 + a\epsilon^\alpha \sin \theta)$ for various ϵ . (a) $(\alpha, a) = (1/2, 1)$, (b) $(\alpha, a) = (1/3, 1/2)$. See the caption of figure 6.

cases of $(\alpha, a) = (1/2, 1)$ in panel (a) and $(\alpha, a) = (1/3, 1/2)$ in panel (b). Again each panel contains the results for three different values of θ ($\theta = \pi/6, \pi/4, \pi/3$). If the asymptotic behaviour shown in (4.5) holds, the double-log plot of $\delta_w^{-1}a|u_r|/\sin 2\theta$ as a function of ϵ for a given (α, a, θ) should approach a line with the slope $1 - \alpha$ as $\epsilon \searrow 0$. In figure 7, we actually observe that each plot tends to approach a line with the slope $1/2$ in panel (a) and a line with the slope $2/3$ in panel (b), independently of θ , as ϵ is reduced. This supports again the asymptotic behaviour of u_r shown in (4.5).

To summarize, the numerical results given above support the presence of the cross-over region between the Knudsen zone and the outer region in which the macroscopic variables behave in the same manner as $\tau/\delta_w \sim (1/2 - \theta/\pi)$ and $u_r/\delta_w \sim (\epsilon/r) \sin 2\theta$.

5. Concluding remarks

In this paper, we considered a slightly rarefied gas confined between two parallel plates with a discontinuous surface temperature distribution and investigated its steady

behaviour. We aimed at extending the conventional GSF theory, which assumes smooth boundary data, to the case in which the boundary temperature has a jump discontinuity, in the simplest case where the boundary is a flat surface. With the aid of rich accumulation of the results known for the case of smooth boundary data, we carried out an asymptotic analysis of the Boltzmann system for small Knudsen numbers based on the matched asymptotic expansion, which employs Sone's asymptotics as the outer solution and a newly introduced kinetic boundary layer (the Knudsen zone) as the inner solution. The analysis was carried out to the first order of the Knudsen number and, in particular, an appropriate form of the 'slip boundary condition' for the flow driven by a discontinuous surface temperature was identified. The main results obtained in this paper are summarized as follows:

- (1) The conventional slip-flow theory, which assumes the smoothness of the boundary data, breaks down near the point where the surface temperature is discontinuous. In this local region (or the Knudsen zone), the solution varies in the scale of the mean free path in both normal and tangential directions to the boundary.
- (2) The half-space boundary-value problem associated with the Knudsen zone for a discontinuous surface temperature over a flat boundary was formulated. The asymptotic form of the solution at far field was derived.
- (3) In the Knudsen zone, the flow velocity decreases with distance in proportion to the reciprocal of the distance. In the far field of the Knudsen zone, the flow velocity has radially diverging or converging streamlines depending on the hotter or colder side.
- (4) The overall flow velocity in the channel is expressed as $u_i = \varepsilon u_{iH1} + O(\varepsilon^2)$ and the essential term u_{iH1} is described by the Stokes equation for an incompressible fluid with the no-slip boundary condition. It also satisfies a singular source/sink condition located at the point of discontinuity, which diverges in approaching the point of discontinuity. The analysis of the half-space problem (i.e. the Knudsen-zone problem) mentioned above determines the multiplicative factor ($\Gamma_Z^{(1)}$) of this singular source/sink condition.
- (5) The result of the direct numerical analysis based on the BGK model for a rarefied gas flow in a square vessel with a discontinuous surface temperature is consistent with that of the asymptotic analysis.

In this way, the 'slip boundary condition' for the flow induced by a discontinuous surface temperature is qualitatively different from those for the thermal-creep or thermal-stress slip flow.

Acknowledgements

This work was supported by JSPS KAKENHI grant no. 17K06146. The authors thank Mr K. Oniyama for his assistance in the numerical analysis carried out in §4. A part of numerical computations was carried out using the supercomputer of ACCMS, Kyoto University.

Declaration of interests

The authors report no conflict of interest.

Appendix A. Derivation of (3.34) and (3.35)

In this appendix, we outline the derivation of (3.34) and (3.35). We focus on the derivation of the Hilbert part, since the derivation of the Knudsen-layer part is

parallel to the derivation of boundary conditions for the Stokes system. Throughout this appendix, the subscript Z0 will be omitted.

Let us assume that, for some small constant $0 < \delta \ll 1$, the length scale of variation is δ^{-1} in the region $(y_1^2 + y_2^2)^{1/2} > \delta^{-1}$, i.e. $\partial\phi/\partial y_i = O(\delta\phi)$. The validity of this assumption is verified if such a solution is obtained. Then, introducing new variables

$$x_i = \delta y_i, \tag{A 1}$$

the velocity distribution function is sought in the form $\phi = \phi(x_1, x_2, \xi_i)$. Then, ϕ satisfies the linearized Boltzmann equation of the form

$$\xi_1 \partial_1 \phi + \xi_2 \partial_2 \phi = \frac{1}{\delta} \mathcal{L}(\phi). \tag{A 2}$$

Thus, δ plays the role of a small Knudsen number and one can seek an asymptotic solution for small values of δ in the form

$$\phi = \phi_H + \phi_K, \tag{A 3a}$$

$$\phi_H = \phi_{H0} + \phi_{H1}\delta + \dots, \tag{A 3b}$$

$$\phi_K = \phi_{K1}\delta + \dots, \tag{A 3c}$$

where ϕ_H is the Hilbert solution and ϕ_K is the Knudsen-layer correction near the boundary $x_1 = 0$. The corresponding macroscopic quantities ω , u_i , τ and P are expressed similarly as

$$h = h_H + h_K, \tag{A 4a}$$

$$h_H = h_{H0} + h_{H1}\delta + \dots, \tag{A 4b}$$

$$h_K = h_{K1}\delta + \dots, \tag{A 4c}$$

where $h = \omega$, u_i , τ and P . Then, the analysis is analogous to § 2 (δ corresponds to ε). In particular, the boundary conditions for the flow velocity and temperature on the lower half of the boundary, $x_1 = 0$ and $x_2 < 0$, are obtained from those on the upper half by replacing τ_w by $-\tau_w$. We shall obtain the asymptotic solution satisfying the required symmetry (3.32).

Order δ^0

We solve (2.11)–(2.12) for $m = 0$ with $\partial_3 = 0$ and $u_{3H0} = 0$ under the boundary conditions

$$u_{iH0} = 0, \quad \tau_{H0} = \pm\tau_w, \quad (x_1 = 0, \pm x_2 > 0), \tag{A 5a}$$

$$u_{iH0} \rightarrow 0, \quad \tau_{H0} \rightarrow \frac{2\tau_w}{\pi}\theta, \quad P_{H0} \rightarrow 0, \quad (r \rightarrow \infty), \tag{A 5b}$$

where $r = \sqrt{x_1^2 + x_2^2}$ and $\theta = \text{Arctan}(x_2/x_1)$. The solution is given by

$$P_{H0} = 0, \quad u_{iH0} = 0, \quad P_{H1} = 0, \quad \tau_{H0} = \frac{2\tau_w}{\pi}\theta, \tag{A 6}$$

where P_{H1} is determined up to an additive constant. Thus, the velocity distribution function is obtained as

$$\phi_{H0} = \frac{2\tau_w}{\pi} \left(\xi_j^2 - \frac{5}{2} \right) \theta. \tag{A 7}$$

There is no Knudsen-layer correction required at this order.

Order δ^1

We solve (2.12) for $m = 1$ with $\partial_3 = 0$ and $u_{3H1} = 0$ under the boundary conditions

$$u_{rH1} = u_{\theta H1} = 0, \quad \tau_{H1} = \mp \frac{2\tau_w c_1^{(0)}}{\pi} \frac{1}{r}, \quad \left(\theta = \pm \frac{\pi}{2}, r > 0\right), \tag{A 8a}$$

$$u_{iH1} \rightarrow 0, \quad \tau_{H1} \rightarrow 0, \quad P_{H1} \rightarrow 0, \quad (r \rightarrow \infty), \tag{A 8b}$$

where u_{rHm} and $u_{\theta Hm}$ are the radial and circumferential components of u_{iHm} in the polar coordinate system centred at the origin. From the last condition of (A 8b), the additive constant in P_{H1} must vanish. Solving the problem, we have

$$P_{H1} = 0, \quad u_{rH1} = \tau_w \frac{\Gamma_Z^{(1)} \sin 2\theta}{r}, \quad u_{\theta H1} = 0, \tag{A 9a}$$

$$P_{H2} = \tau_w \frac{2\gamma_1 \Gamma_Z^{(1)}}{r^2} \sin 2\theta, \quad \tau_{H1} = -\frac{2}{\pi} \tau_w c_1^{(0)} \frac{\sin \theta}{r}, \tag{A 9b}$$

where $\Gamma_Z^{(1)}$ is an undetermined constant and P_{H2} is determined up to an additive constant. From (2.43), the velocity distribution function is given by

$$\frac{\phi_{H1}}{\tau_w} = 2\xi_r \frac{\Gamma_Z^{(1)} \sin 2\theta}{r} - \left(\xi_j^2 - \frac{5}{2}\right) \frac{2}{\pi} c_1^{(0)} \frac{\sin \theta}{r} - \frac{2}{\pi} A(\xi) \frac{\xi_\theta}{r}, \tag{A 10a}$$

$$\frac{\phi_{K1}}{\tau_w} = -\frac{2}{\pi} \frac{1}{x_2} \varphi_1^{(0)}(y_1, \xi_1, \xi), \tag{A 10b}$$

where $\xi = (\xi_j^2)^{1/2}$ and $y_1 = x_1/\delta$. The Knudsen-layer corrections for the macroscopic quantities are summarized as

$$u_{rK1} = u_{\theta K1} = 0, \quad \omega_{K1} = -\frac{2}{\pi} \frac{1}{x_2} \Omega_1^{(0)}(y_1), \tag{A 11a}$$

$$\tau_{K1} = -\frac{2}{\pi} \frac{1}{x_2} \Theta_1^{(0)}(y_1), \quad P_{K1} = -\frac{2}{\pi} \frac{1}{x_2} (\Omega_1^{(0)}(y_1) + \Theta_1^{(0)}(y_1)). \tag{A 11b}$$

Order δ^2

For the purpose of the present study, we do not need the information of the far-field asymptotics to the order δ^2 . However, it is important for the numerical analysis as well as for a theoretical insight. Therefore, we present the result.

If we continue the analysis in § 2 to the order of ε^2 or referring to chap. 3 of Sone (2007) (or to Takata & Hattori (2012)), the boundary conditions on $x_1 = 0$ are given by

$$u_{rH2} = \pm 2\tau_w \frac{\Gamma_Z^{(1)} b_1^{(1)} + \frac{c_1^{(0)} b_2^{(1)} + b_3^{(1)}}{\pi}}{r^2}, \quad u_{\theta H2} = 0, \quad \tau_{H2} = 0, \quad \left(\theta = \pm \frac{\pi}{2}, r > 0\right), \tag{A 12a}$$

$$u_{iH2} \rightarrow 0, \quad \tau_{H2} \rightarrow 0, \quad P_{H2} \rightarrow 0, \quad (r \rightarrow \infty). \tag{A 12b}$$

The last condition of (A 12b) determines the additive constant in P_{H2} to be zero. Finding solutions to (2.12) for $m=2$ with $\partial_3=0$ and $u_{3H2}=0$ under these conditions, we have

$$\frac{u_{rH2}}{\tau_w} = \frac{-3\Gamma_Z^{(2)}(\sin 3\theta + \sin \theta) + 2\left(\Gamma_Z^{(1)}b_1^{(1)} + \frac{c_1^{(0)}b_2^{(1)} + b_3^{(1)}}{\pi}\right)\sin \theta}{r^2}, \tag{A 13a}$$

$$\frac{u_{\theta H2}}{\tau_w} = \frac{\Gamma_Z^{(2)}(\cos 3\theta + 3\cos \theta) - 2\left(\Gamma_Z^{(1)}b_1^{(1)} + \frac{c_1^{(0)}b_2^{(1)} + b_3^{(1)}}{\pi}\right)\cos \theta}{r^2}, \tag{A 13b}$$

$$\frac{\tau_{H2}}{\tau_w} = \frac{\Lambda_Z^{(2)}}{r^2} \sin 2\theta, \tag{A 13c}$$

where $\Gamma_Z^{(2)}$ and $\Lambda_Z^{(2)}$ are undetermined constants. It is worth noting that the flow velocity is a special case of plane flows around a corner (Moffatt 1964). The velocity distribution function is then given by

$$\begin{aligned} \frac{\phi_{H2}}{\tau_w} = & \frac{2\gamma_1\Gamma_Z^{(1)}}{r^2} \sin 2\theta + \left(\xi_j^2 - \frac{5}{2}\right) \frac{\Lambda_Z^{(2)}}{r^2} \sin 2\theta \\ & - 2\Gamma_Z^{(2)} \frac{3\xi_r(\sin 3\theta + \sin \theta) - \xi_\theta(\cos 3\theta + 3\cos \theta)}{r^2} \\ & + 4\left(\Gamma_Z^{(1)}b_1^{(1)} + \frac{c_1^{(0)}b_2^{(1)} + b_3^{(1)}}{\pi}\right) \frac{\xi_r \sin \theta - \xi_\theta \cos \theta}{r^2} \\ & - \frac{2}{\pi}c_1^{(0)} \left(\frac{\xi_r \sin \theta - \xi_\theta \cos \theta}{r^2}\right) A(\xi) \\ & + \Gamma_Z^{(1)} \left(\frac{(\xi_r^2 - \xi_\theta^2) \sin 2\theta - 2\xi_r\xi_\theta \cos 2\theta}{r^2}\right) B(\xi) + \frac{4}{\pi} \frac{\xi_r\xi_\theta}{r^2} F(\xi), \tag{A 14a} \end{aligned}$$

$$\frac{\phi_{K2}}{\tau_w} = \frac{\xi_2}{x_2^2} \left(2\Gamma_Z^{(1)}\varphi_1^{(1)}(y_1, \xi_1, \xi) + \frac{2}{\pi}c_1^{(0)}\varphi_2^{(1)}(y_1, \xi_1, \xi) + \frac{2}{\pi}\varphi_3^{(1)}(y_1, \xi_1, \xi)\right). \tag{A 14b}$$

The Knudsen-layer corrections for the macroscopic quantities are summarized as

$$\frac{u_{rK2}}{\tau_w} = \frac{2}{x_2^2} \left(\Gamma_Z^{(1)}Y_1^{(1)}(y_1) + \frac{c_1^{(0)}Y_2^{(1)}(y_1) + Y_3^{(1)}(y_1)}{\pi}\right) \sin \theta, \tag{A 15a}$$

$$\frac{u_{\theta K2}}{\tau_w} = \frac{2}{x_2^2} \left(\Gamma_Z^{(1)}Y_1^{(1)}(y_1) + \frac{c_1^{(0)}Y_2^{(1)}(y_1) + Y_3^{(1)}(y_1)}{\pi}\right) \cos \theta, \tag{A 15b}$$

$$\omega_{K2} = \tau_{K2} = P_{K2} = 0. \tag{A 15c}$$

Assembling the above results according to (A 3)–(A 4) and taking account the relations $\delta/x_2 = 1/y_2$ and $\delta/r = 1/\tilde{r}$, we obtain (3.34) and (3.35).

REFERENCES

- ANDRIES, P., TALLEC, P. L., PERLAT, J.-P. & PERTHAME, B. 2000 The Gaussian-BGK model of Boltzmann equation with small Prandtl number. *Eur. J. Mech. (B/Fluids)* **19** (6), 813–830.
- AOKI, K., SONE, Y. & MASUKAWA, N. 1995 A rarefied gas flow induced by a temperature field. In *Rarefied Gas Dynamics* (ed. J. Harvey & G. Lord), pp. 35–41. Oxford University Press.
- AOKI, K., TAKATA, S., AIKAWA, H. & GOLSE, F. 2001 A rarefied gas flow caused by a discontinuous wall temperature. *Phys. Fluids* **13** (9), 2645–2661; erratum: **13**, 3843 (2001).
- AOKI, K., TAKATA, S. & TOMOTA, T. 2014 A force acting on an oblate spheroid with discontinuous surface temperature in a slightly rarefied gas. *J. Fluid Mech.* **748**, 712–730.
- BAIER, T., HARDT, S., SHAHABI, V. & ROOHI, E. 2017 Knudsen pump inspired by Crookes radiometer with a specular wall. *Phys. Rev. Fluids* **2**, 033401.
- BAIER, T., TIWARI, S., SHRESTHA, S., KLAR, A. & HARDT, S. 2018 Thermophoresis of Janus particles at large Knudsen numbers. *Phys. Rev. Fluids* **3**, 094202.
- BARDOS, C., CAFLISCH, R. E. & NICOLAENKO, B. 1986 The Milne and Kramers problems for the Boltzmann equation of a hard sphere gas. *Commun. Pure Appl. Maths* **39** (3), 323–352.
- BHATNAGAR, P. L., GROSS, E. P. & KROOK, M. 1954 A model for collision processes in gases. I. Small amplitude processes in charged and neutral one-component systems. *Phys. Rev.* **94**, 511–525.
- BRULL, S. 2015 An ellipsoidal statistical model for gas mixtures. *Commun. Math. Sci.* **13** (1), 1–13.
- CORON, F., GOLSE, F. & SULEM, C. 1988 A classification of well-posed kinetic layer problems. *Commun. Pure Appl. Maths* **41** (4), 409–435.
- DONKOV, A. A., TIWARI, S., LIANG, T., HARDT, S., KLAR, A. & YE, W. 2011 Momentum and mass fluxes in a gas confined between periodically structured surfaces at different temperatures. *Phys. Rev. E* **84**, 016304.
- DYKE, M. V. 1975 *Perturbation Methods in Fluid Mechanics*. Parabolic.
- HOLWAY, J. 1966 New statistical models for kinetic theory: methods of construction. *Phys. Fluids* **9** (9), 1658–1673.
- KENNARD, E. H. 1938 *Kinetic Theory of Gases*. McGraw-Hill.
- KETSDEVER, A., GIMELSHEIN, N., GIMELSHEIN, S. & SELDEN, N. 2012 Radiometric phenomena: from the 19th to the 21st century. *Vacuum* **86**, 1644–1662.
- LI, Q., LIANG, T. & YE, W. 2014 Knudsen torque: a rotational mechanism driven by thermal force. *Phys. Rev. E* **90**, 033009.
- LOTFIAN, A. & ROOHI, E. 2019 Radiometric flow in periodically patterned channels: fluid physics and improved configurations. *J. Fluid Mech.* **860**, 544–576.
- LOYALKA, S. K. 1969 Thermal transpiration in a cylindrical tube. *Phys. Fluids* **12**, 2301–2305.
- MOFFATT, H. K. 1964 Viscous and resistive eddies near a sharp corner. *J. Fluid Mech.* **18** (1), 1–18.
- NIIMI, H. 1971 Thermal creep flow of rarefied gas between two parallel plates. *J. Phys. Soc. Japan* **30** (2), 572–574.
- OHWADA, T., SONE, Y. & AOKI, K. 1989a Numerical analysis of the Poiseuille and thermal transpiration flows between two parallel plates on the basis of the Boltzmann equation for hard-sphere molecules. *Phys. Fluids A* **1** (12), 2042–2049; erratum: **2**, 639 (1990).
- OHWADA, T., SONE, Y. & AOKI, K. 1989b Numerical analysis of the shear and thermal creep flows of a rarefied gas over a plane wall on the basis of the linearized Boltzmann equation for hard-sphere molecules. *Phys. Fluids A* **1** (9), 1588–1599.
- SHARIPOV, F. 2002 Application of the Cercignani-Lampis scattering kernel to calculations of rarefied gas flows. III. Poiseuille flow and thermal creep through a long tube. *Eur. J. Mech. (B/Fluids)* **22** (2), 145–154.
- SONE, Y. 1966 Thermal creep in rarefied gas. *J. Phys. Soc. Japan* **21**, 1836–1837.
- SONE, Y. 1969 Asymptotic theory of flow of rarefied gas over a smooth boundary I. In *Rarefied Gas Dynamics* (ed. L. Trilling & H. Y. Wachman), vol. 1, pp. 243–253. Academic Press.
- SONE, Y. 1971 Asymptotic theory of flow of rarefied gas over a smooth boundary II. In *Rarefied Gas Dynamics* (ed. D. Dini), vol. 2, pp. 737–749. Editrice Tecnico Scientifica.
- SONE, Y. 2002 *Kinetic Theory and Fluid Dynamics*. Birkhäuser.

- SONE, Y. 2007 *Molecular Gas Dynamics: Theory, Techniques, and Applications*. Birkhäuser.
- SONE, Y. & YAMAMOTO, K. 1968 Flow of rarefied gas through a circular pipe. *Phys. Fluids* **11**, 1672–1678; erratum: **13**, 1651 (1970).
- SONE, Y. & YOSHIMOTO, M. 1997 Demonstration of a rarefied gas flow induced near the edge of a uniformly heated plate. *Phys. Fluids* **9**, 3530–3534; supplementary video: Kyoto University Research Information Repository. Available at: <http://hdl.handle.net/2433/122357>.
- SUGIMOTO, H. & SONE, Y. 2005 Vacuum pump without a moving part by thermal edge flow. In *Rarefied Gas Dynamics* (ed. M. Capitelli), pp. 168–173. AIP.
- TAGUCHI, S. 2015 Asymptotic theory of a uniform flow of a rarefied gas past a sphere at low Mach numbers. *J. Fluid Mech.* **774**, 363–394.
- TAGUCHI, S. & AOKI, K. 2012 Rarefied gas flow around a sharp edge induced by a temperature field. *J. Fluid Mech.* **694**, 191–224.
- TAGUCHI, S. & AOKI, K. 2015 Motion of an array of plates in a rarefied gas caused by radiometric force. *Phys. Rev. E* **91**, 063007.
- TAGUCHI, S. & SUZUKI, T. 2017 Asymptotic far-field behavior of macroscopic quantities in a problem of slow uniform rarefied gas flow past a sphere. *Phys. Rev. Fluids* **2**, 113401.
- TAKATA, S. & FUNAGANE, H. 2011 Poiseuille and thermal transpiration flows of a highly rarefied gas: over-concentration in the velocity distribution function. *J. Fluid Mech.* **669**, 242–259.
- TAKATA, S. & HATTORI, M. 2012 Asymptotic theory for the time-dependent behavior of a slightly rarefied gas over a smooth solid boundary. *J. Stat. Phys.* **147** (6), 1182–1215.
- TAKATA, S. & HATTORI, M. 2015 Numerical data for the generalized slip-flow theory. Kyoto University Research Information Repository. Available at: <http://hdl.handle.net/2433/199811>.
- TAKATA, S., HATTORI, M. & HASEBE, T. 2016 Slip/jump coefficients and Knudsen-layer corrections for the ES model in the generalized slip-flow theory. *AIP Conf. Proc.* **1786** (1), 040004.
- WELANDER, P. 1954 On the temperature jump in a rarefied gas. *Ark. Fys.* **7**, 507–553.